UNIVERSITY
OF MICHIGAN
FEB 2 1953
PHYSICS
LIBRARY

REGISTERED NO. M. 3121

PROCEEDINGS
OF THE
INDIAN ACADEMY
OF SCIENCES

VOL. XXXVI] *SECTION A* [NO. 2

AUGUST 1952

Price Rs. 2 or 3 Sh. *Annual Subscription Rs. 18*

PRINTED AT THE BANGALORE PRESS, BANGALORE CITY, BY G. SRINIVASA RAO, SUPERINTENDENT, AND PUBLISHED BY THE INDIAN ACADEMY OF SCIENCES, BANGALORE.

PRODUCTION AND INTERACTION OF MESONS AT VERY HIGH ENERGIES

By D. Lal, Yash Pal, B. Peters and M. S. Swami

(*Tata Institute of Fundamental Research, Bombay*-1)

Received June 13, 1952

(Communicated by Professor H. J. Bhabha, F.A.SC., F.R.S.)

Abstract

A shower containing ~ 360 charged and neutral shower particles produced by a magnesium nucleus of 2×10^{14} e.v. provides a source of mesons whose interactions have been studied over an aggregate track length of about 3 meters in emulsion. It is first shown that in very large showers not only the incident energy can be determined but also the energy of the shower particles. The angular distribution of the shower particles agrees closely and their multiplicity is consistent with Fermi's theory.

It is shown that the interaction cross-section of charged shower particles is geometric and that at an energy $\epsilon \sim 1000\,\mu c^2$ they produce on the average 5 to 6 mesons. The mesons are preferentially emitted in the backward direction in the reference system in which the momentum of the incident meson balances that of a nucleon in the target. The excitation produced in the target nucleus is much lower than in nucleon-produced showers of comparable multiplicity.

The charged mesons are *not* emitted in pairs by a heavier meson of short lifetime.

Charged shower particles as well as electrons produce electron-positron pairs with a cross-section of the order of that predicted by theory.

The number of neutral mesons decaying into γ-rays in a time $\leqslant 10^{-14}$ sec. is nearly equal to the number of charged shower particles.

There exists evidence for the emission of neutral particles, different from neutrons, capable of producing meson showers.

The energy balance of the event suggests that a few shower particles carry an appreciable fraction of the total energy.

I. Introduction

The main subject of this paper is the study of a narrow beam of ~ 360 charged and neutral particles of high energy confined to a cone of 7·4° half

aperture. This cone lies inside a large stack of photographic emulsions in which the path length of each particle exceeds 9 cm. The aggregate track length in terms of distance, weight of material traversed and radiation units is therefore appreciable and permits the observation of phenomena related to the lifetime, the nuclear interactions and the electromagnetic interactions of the shower particles.

In Section II, we discuss an extension of previously used methods, applicable to very large showers, for the determination of the energy of the primary and the energy of the secondary particles. The latter is obtained under the simplifying assumption that the great majority of the shower particles is fairly mono-energetic in the centre of mass system of the collision. The results obtained justify the belief that this assumption is a reasonably good approximation but that it should not be amplified to mean that the most probable and the average energy of the shower particles are equal.

In Section III, we consider the charged shower particles and the information which can be derived from their angular distribution and from the interactions which they initiate.

In Section IV, we consider the neutral shower particles, assumed to be responsible for the appearance of the large soft component in the shower whose development can be studied in great detail. We also consider two cases of nuclear interactions induced by neutral shower particles.

Section V deals with the charge and energy balance of the event.

II. The Energy Determination of Primary and Secondary Particles in Large Meson Showers

In order to analyse the properties of shower particles from their decay products and nuclear interactions it is essential to obtain an accurate knowledge of their velocity as a function of their angle of emission.

In this section we will show that for very large showers it is possible to obtain the energy of the primary as well as the velocity of the shower particles and their angular distribution in the C-system from the angular distribution of the shower particles in the laboratory system and that for the largest shower investigated it is possible to determine these quantities with reasonable accuracy.

We shall first show in subsection A that in large showers, the shower particles are produced with relativistic velocity in the C-system and that an upper limit for the primary energy is directly obtainable from the main characteristics of their angular distribution in the L-system.

In subsection B we will show that, if the number of shower particles is so large that statistically significant numbers appear in small angular intervals, the details of the angular distribution together with the requirement that in the C-system it is symmetric with respect to a plane perpendicular to the direction of motion, determines both the energy of the primary particles and the velocity of the shower particles. This analysis is carried out in detail on a shower containing ~ 200 charged shower particles.

A. An Upper Limit for the Primary Energy

In the laboratory system (L-system) the velocity and energy (in units of rest mass) of the colliding nucleons and shower particles respectively is designated by β, γ, β_0, γ_0. A bar is placed over the symbols when they refer to the system in which incident and target nucleons have equal and opposite momenta (C-system). The ratio of the velocities of the nucleons and shower particles in the C-system is designated by $\bar{\beta}/\bar{\beta}_0 = m$ and the angles of emission in the L- and C-systems are θ and ϑ respectively.

The transformation between angles in the two systems is then given by

$$\bar{\gamma} \tan \theta = \frac{\sin \vartheta}{m + \cos \vartheta}. \tag{1}$$

If $m \leqslant 1$ there exists a one to one correspondence between the angles of emission in both systems and to the angle θ_f defining a cone in the L-system which contains the fraction f of all shower particles there corresponds an angle ϑ_f defining a similar cone in the C-system. For $m = 1$ the requirement of symmetry of emission in the C-system ($\vartheta_f = \pi - \vartheta_{1-f}$) leads then to the relation determining the energy per nucleon of the incident primary:

$$\frac{E}{MC^2} = \gamma \approx 2\bar{\gamma}^2 = 2 \cot \theta_f \cot \theta_{1-f}^{*}. \tag{2}$$

The product $\cot \theta_f \cot \theta_{1-f}$ has been determined for three large showers and is given in Table I. The errors indicated in the last column are estimates of the errors in the determination of θ_f, θ_{1-f} based on the track density in each angular interval. It is seen that the product is indeed a constant over a large range of values of f. Thus it shows that $\bar{\beta}/\bar{\beta}_0$ is close to unity and that the shower particles are emitted with relativistic velocities in the C-system. There is however a deviation for $f \lesssim 0{\cdot}1$ in showers No. 2 and 3. In shower No. 2 the angle $\theta_{0{\cdot}1}$ contains only 5–6 shower particles and

* Eq. 2 implies that all shower particles are produced in C-systems moving with equal velocities. This assumption is probably justified for energetic showers of small angular aperture since a second collision in the same nucleus will consist of an encounter in which all the products of the first collision collide again with a single nucleon.

large fluctuations may be expected. In shower No. 3 however the deviation is significant and shows that eq. 2 does not determine the primary energy correctly; it does, however, give an *upper* limit to the primary energy as shown below.

TABLE I

Shower No.	Primary Nucleus	Number of charged shower particles n_s	f	θ°_f	θ°_{1-f}	$\frac{\epsilon}{MC^2} = \frac{}{2 \cot \theta_f \cot \theta_{1-f}}$
1	He	59	·5	4·75	4·75	292± 18
			·4	2·85	8·55	268± 15
			·3	1·70	13·95	271± 19
			·2	0·89	25·16	274± 15
			·1	0·65	32·33	278± 15
2	He	57	·5	3·40	3·40	570± 30
			·4	2·35	5·15	545± 30
			·3	1·55	8·15	518± 30
			·2	0·85	13·2	575± 40
			·1	0·45	22·2	624± 50
3	Mg	210	·5	0·735	0·735	12100± 250
			·4	0·388	1·134	14900± 350
			·3	0·267	1·920	12800± 350
			·2	0·175	2·900	12900± 400
			·1	0·0738	4·470	20100±3000

B. Determination of the Energy of Shower Particles

Since all the showers considered in this paper have large primary energy ($\bar{\beta} \approx 1$) the value of $m = \bar{\beta}/\bar{\beta}_0$ cannot be significantly smaller than unity. It can however be larger than unity if the mesons are emitted in the C-system with relatively low velocities. In this case we have no longer a one to one correspondence between the angles of emission in the two systems.

One half of all mesons will in the C-system be emitted with angles $\vartheta < \pi/2$ and therefore appear in the L-system in the cone defined by $\bar{\gamma} \tan \theta = \frac{1}{m}$. In addition however this same cone in the L-system also contains mesons which in the C-system are emitted in the angular interval $-1 < \cos \vartheta < -2m/(m^2+1)$. Therefore, if $\theta_{\frac{1}{2}}$ defines the cone in the L-system which contains half the shower particles, we must have

$$\bar{\gamma} \tan \theta_{\frac{1}{2}} \leqslant \frac{1}{m} \leqslant 1 \text{ or } \gamma \leqslant 2 \cot^2 \theta_{\frac{1}{2}}.$$

Thus the energies obtained in Table I represent an upper limit to the true primary energies.

In order to find the correct value of the primary energy as well as the velocity of the shower particles we have to make a more detailed study of the angular distribution of shower particles in the L-system. Such a study is only warranted if the multiplicity is very high; we confine therefore our analysis to shower No. 3.

The two parameters appearing in equation 1 are:

The energy of the primary nucleon ($\bar{\gamma}$) and

The ratio of its velocity to that of the shower particles (m).

One relation between these parameters is provided by the condition that the maximum spread of the shower is determined by

$$\bar{\gamma} \tan \theta_m = \frac{1}{\sqrt{m^2 - 1}} \tag{3}$$

from eq. 1. The second required relation is obtained from the condition that the transformation of the angular distribution from the L-system to the C-system must produce an angular distribution which is symmetric about the plane defined by $\cos \vartheta = 0$.

C. Description of the Shower No. 3 and Evaluation of its Energy

This shower is produced by a magnesium nucleus in the glass of a stack of 80 plates coated with NT4 emulsions 230–240 μ thick. The shower particles emerge into the first emulsion after traversing 5·1 mm. of glass. All the particles which emerge have minimum ionization. The absence of any relativistic α-particle or heavier fragment indicates that the destruction of the primary nucleus was complete and therefore presumable a large number of nucleon-nucleon collisions took place. 207 Charged shower particles emerging from the glass where the event took place are contained in a cone whose half angle of aperture is 7·4°. Survey of an area 4 times larger than the intersection of this cone with the first emulsion resulted in three additional tracks close to the boundary of the cone. The angular measurements were carried out at a distance of 7080 μ from the origin. The resolution obtained was better than 5×10^{-4} radians. The shower left the stack after passing through 24 emulsions. The total distance from origin to exit is 9·2 cm. of which 66·7% were taken up by glass, 15% by emulsion and the rest by air gaps. The emulsion represented however 50% of the material when expressed in γ-ray conversion units and 21% when expressed in units of the mean free path for nuclear interactions.

Fig. 1 shows the track of the primary nucleus and the appearance of the core area in the first emulsion. Fig. 2 shows the angular distribution

SHOWER No. 3
Integral Angular Distribution in Laboratory System

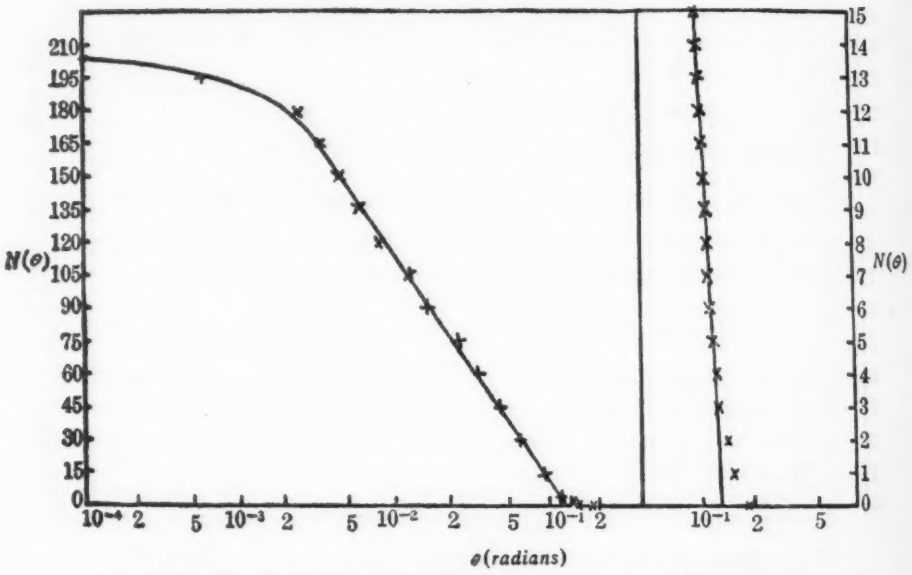

FIG. 2. Showing $N(\theta)$ the number of tracks emitted at an angle greater than θ in the Laboratory System. Plot on the right shows the tail end of the distribution in detail.

of shower particles in the L-system. From this distribution we determine the maximum width of the shower $\tan\theta_m = 0{\cdot}130$ ($\theta_m = 7{\cdot}4°$). There are three additional tracks outside this cone ($\theta = 8{\cdot}1°$; $8{\cdot}8°$; and $11{\cdot}1°$) which may be due to shower particles of more than average velocity. We shall show however that the result is not seriously affected if we take $\theta_m = 11{\cdot}1°$ instead of $7{\cdot}4°$. With the help of (eq. 1, 3) we can convert the angular distribution in the L-system into an angular distribution in the C-system using various values for $\bar{\beta}/\bar{\beta}_0 = m$. Table II shows the number of particles which appear in the forward and backward directions in different angular intervals in the C-system.

A symmetrical distribution is obtained for $m = 1{\cdot}007$ which together with $\tan\theta_m = 0{\cdot}13$ gives for the energy of the primary $\bar{\gamma} = 65$ $\left(\gamma = \frac{\epsilon}{MC^2} = 8430\right)$ and for the energy of the shower particles $\bar{\gamma}_0 = 8{\cdot}4$. If we choose $\theta_m = 11{\cdot}1°$ instead of $7{\cdot}4°$ and make an identical calculation we obtain symmetry for $m = 1{\cdot}003$ corresponding to $\frac{\epsilon}{MC^2} = 8700$ and $\bar{\gamma}_0 = 12{\cdot}5$. Fig. 2 however suggests that the former choice for θ_m is more accurate.

TABLE II

$m =$	1·002		1·004		1·006		1·007		1·008		1·010		1·012	
	Forw.	Backw.	Forw.	Backw.	Forw.	Backw.	Forw.	Backw.	Forw.	Backw.	Forw.	Backw.	Forw.	Backw.
$\frac{1}{m} < \lvert \cos\vartheta \rvert < \cdot 95$	17	43	11	24	10	18	12	14	14	14	19	10	21	11
$\cdot 95 < \lvert \cos\vartheta \rvert < \cdot 85$	7	27	22	30	25	26	26	25	32	21	28	21	32	19
$\cdot 85 < \lvert \cos\vartheta \rvert < \cdot 75$	14	7	13	16	19	13	19	14	14	14	16	16	15	14
$\frac{1}{m} < \lvert \cos\vartheta \rvert < \cdot 75$	38	77	46	70	54	57	57	53	60	49	63	47	68	44

Thus the energy of the primary nucleus and of the shower particles are fairly accurately determined by the angular distribution in the L-system. The magnesium nucleus which produced the shower had an energy of $7{\cdot}8 \times 10^{12}$ eV. per nucleon or a total energy of $1{\cdot}9 \times 10^{14}$ eV. The shower particles are produced in the C-system with energies of order $10\,\mu c^2$.

We can now plot the angular distribution of the shower particles in the C-system except for the small interval $-1 < \cos\vartheta < -\frac{1}{m}$ or $173{\cdot}2° < \vartheta < 180°$. The tracks belonging to this interval are spread over our entire distribution in the L-system. Their number should be equal to the number of tracks emitted in the interval $0 < \vartheta < 6{\cdot}8°$. There are 18 tracks in this interval. We have therefore added 18 tracks in Fig. 3 to the other tracks emitted close to the backward direction and indicated this correction by a shaded segment in the histogram. The curve in Fig. 3 represents the angular distribution for median impact parameter as derived by Fermi (1951). The agreement between the theoretical and experimental angular distributions is very close.

The velocity of the shower particles in the L-system is obtained from the relation

$$\gamma_0 = \bar{\gamma}_0 \bar{\gamma} + \sqrt{\bar{\gamma}_0^2 - 1}\ \sqrt{\bar{\gamma}^2 - 1} \cos\vartheta$$

and is plotted in Fig. 4.

III. Properties of the Charged Shower Particles

A. The Absence of Zeta-Mesons

It has been suggested (Danysz, *et al.*, 1952) that one of the particles emitted in high energy collisions is a neutral meson of very short lifetime

SHOWER No. 3
Angular Distribution in C-System

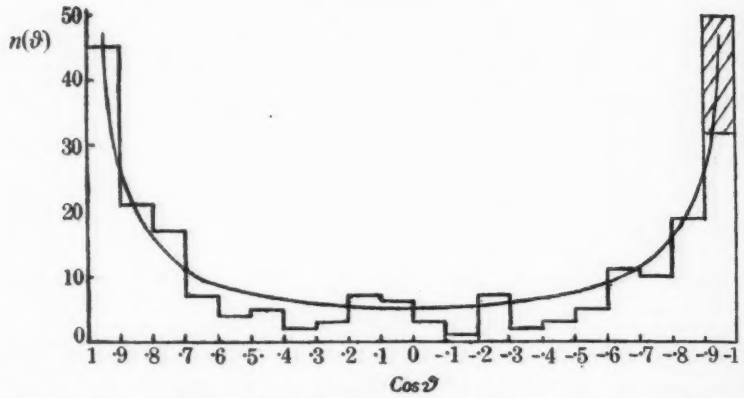

FIG. 3. The histogram gives the angular distribution of shower particles in the C-System. The shaded area indicates the contribution from the C.M. angle corresponding to $-\frac{1}{m} < \cos\vartheta < -1$. The smooth curve is Fermi's result for the median value of impact parameter.

SHOWER No. 3
Energy Distribution in Laboratory System

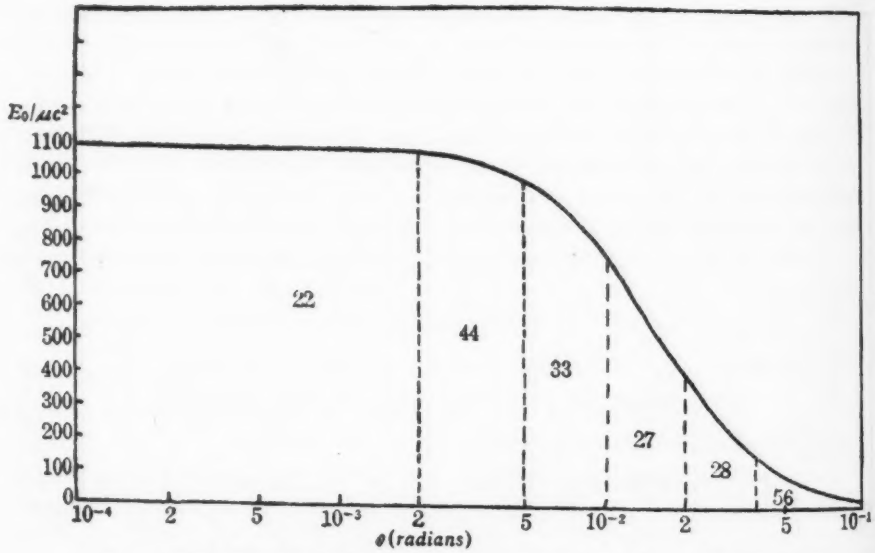

FIG. 4. Plot giving the energy of the shower particles in units of their rest mass as a function of their angle of emission in the Laboratory System. Inset figures indicate the number of particles in different energy intervals.

($\tau_0 < 10^{-14}$ sec.) disintegrating into a pair of charged pions, the Q value of the reaction being of the order of 3 MeV. Shower No. 3 affords an opportunity to test this hypothesis. If Zeta mesons were produced we should observe pairs of charged particles whose angular separation is less than

$$\alpha_{max.} = \frac{2\sqrt{Q}}{\gamma_0},$$

where Q is the excess in the mass of the parent particle in units of the mass of the daughter product. We know the value of γ_0 as a function of angular distance from the shower core (Fig. 4). If the Q value is 3 MeV. and the product particles are not lighter than pions, the largest possible separation of the doublets at a distance of 7·1 mm. from the origin is 1·9 μ near the centre of the core and 24·6 μ at a distance of 355 μ from the shower axis. We exclude the region within 35 μ from the shower axis where the track density is so high as to make accidental coincidences probable. In the region from 35 μ to 355 μ from the axis the mean distance between tracks is 4 to 9 times the expected *maximum* separation for doublets. We find among a total of 101 shower particles six pairs which are close enough to be the products of a Zeta-meson. Since as shown in Section III we expect to see in this region six electron-positron pairs from γ-rays converted in the material which separates the emulsion from the origin, it seems certain, that the shower particles observed in this event are not the decay products of a shortlived neutral parent particle unless the Q value of the reaction is very much higher than the assumed value of 3 MeV.

B. The Interaction Cross-Section of Charged Shower Particles

We have surveyed most of the shower area in 23 emulsions. The aggregate track length of charged shower particles in the surveyed area was 201 cm. or 805 gr./cm.^{2} In this region we found 8 nuclear interactions produced by charged shower particles. (In addition there were 2 nuclear interactions produced by neutral particles in which the distribution of shower particles clearly indicated that the primary originated in the main event.) If the charged shower particles have an interaction cross-section corresponding to the geometrical area of the target nuclei then we expect to see 8·6 collisions produced by charged shower particles ($\lambda = 93$ gr./cm.^{2} in emulsion). We therefore conclude that the most and probably all the charged particles created in the original event have geometric interaction cross-section.

C. The Nature of the Secondary Interactions

Since the original shower must, in addition to mesons, contain approximately 20 protons and 20 neutrons (representing the nuclear matter of the

primary and the target nucleus) we expect about one interaction due to protons and one due to neutrons.

Most of the secondary interactions initiated by charged particles must therefore be due to mesons.

A total of 56 additional charged shower particles are produced in nine secondary interactions. (In the tenth interaction the charged particle passes through the nucleus undeviated.) The appearance of the showers differs in two respects from " ordinary " showers (which are presumably mostly produced by nucleons). Heavy prongs are comparatively rare and the angular aperture of the showers appears to be comparatively large.

(α) *Excitation of the Target Nucleus by Fast Mesons*

Table III gives the number of shower particles (n_s) as well as the number of non-relativistic singly charged particles and evaporation fragments (N_h) in each of the secondary interactions. In the last column we have listed the number of heavy tracks in " ordinary " showers of equal multiplicity as obtained by Camerini, *et al.* (1951). Following the notation of these authors we use the subscripts p and n for showers produced by charged and

TABLE III

Prong Distribution in Secondary Meson Showers

Star No.	Number of shower particles n_s	Number of prongs N_h	Average number of heavy prongs in " ordinary " showers
1	4_p	1	11
2	4_n	1	11
3	5_p	3	12
4	5_p	8	12
5	5_n	0	12
6	6_p	1	12
7	8_p	5	13
8	8_p	9	13
9	11_p	2	14
Total ..	56	30	110

neutral particles respectively. The data in Table III strongly suggest that meson-produced meson showers lead to much lower excitation of the target nucleus than showers of equal multiplicity produced by nucleons. Showers with zero or one heavy track (jet type showers) seem to be common. They have frequently been interpreted as due to collision with protons or glancing collisions with heavy nuclei. It appears however that at least in some cases the absence of heavy tracks may be connected with the nature of the primary particle rather than with the nature of the target nucleus or the geometry of the collision.

(β) The Angular Distribution of Shower Particles in Meson Produced Showers

The angle of emission and therefore the value γ_0 of each of the particles producing secondary stars is known from Fig. 4. If we think of the secondary showers as being produced in a collision between a meson and a nucleon in the target nucleus we can define a reference system (C′-system) in which the total momentum of the secondary collision is zero. The velocity of this system is given by $(1-\bar{\beta}'^2)^{-1}=\bar{\gamma}^2\approx\frac{\gamma_0\mu}{2\,\mathrm{M}}$ and the relation between the angles of the shower particles in the L-system and C′-system respectively is given by

$$\sqrt{\frac{\gamma_0\mu}{2\,\mathrm{M}}}\,\tan\theta'=\frac{\sin\vartheta'}{\bar{\beta}'/\bar{\beta}_0'+\cos\vartheta'}$$

Here μ is the mass of the incident meson, M the mass of the nucleon and $\bar{\beta}_0'$ the velocity of the secondary shower particles in the C′-system. Since in these collisions $\bar{\beta}'\approx 1$ the ratio of velocities of the C′-system to that of the secondary particles in the C′-system $\bar{\beta}'/\bar{\beta}_0'$ must be larger or equal to unity. Using again the argument presented in Section II we find that, if half the shower particles in the C′-system are emitted with angles $\vartheta'<\pi/2$, then more than half the particles must in the L-system be emitted within the laboratory angle defined by

$$\frac{\gamma_0}{2}\tan^2\theta'<\mathrm{M}/\mu.$$

Since in each secondary star the value of γ_0 and the angle of emission of the shower particles (θ') is known, we can, assuming various values of M/μ, obtain an upper limit for the number of secondary shower particles which in the C′-system are emitted into the forward hemisphere. We find that less than half of the 56 secondary shower particles are emitted into the forward hemisphere unless we assume that the average mass of the incident meson is less than 7% of the proton mass.

Because as shown before the excitation produced in the target nucleus is generally small and few if any slow particles are emitted, it is unlikely that the angular distribution of the shower particles is greatly widened by scattering inside the target nucleus. Our result therefore seems to indicate that in meson produced meson showers particularly in those of high multiplicity the shower-particles are in the C′-system predominantly emitted in the backward direction. Some of these showers are reproduced in Fig. 5.

SHOWER No. 3

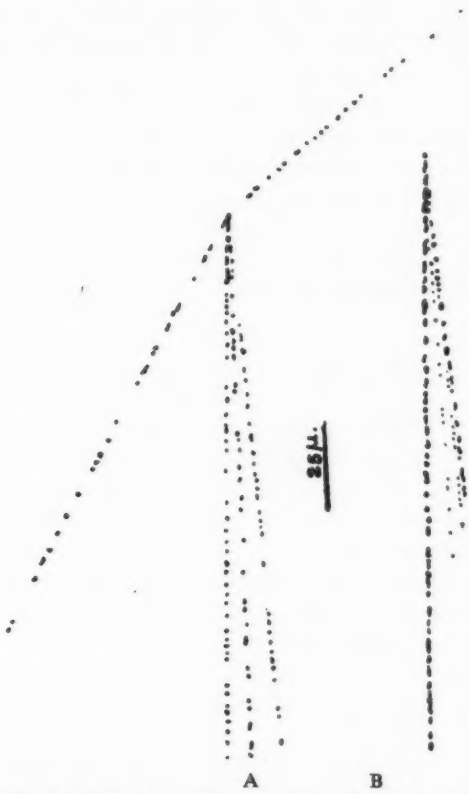

FIG. 5 A. Facsimile drawing of a secondary event of the type $0+5_n$ caused by a neutral shower particle in the original shower.

FIG. 5 B. Facsimile drawing of a secondary event of the type $1+4_n$ caused by a neutral shower particle in the original shower.

The meson production by mesons may perhaps be thought of as a process in which the incident meson interacts only locally in passing through the meson cloud surrounding each nucleon and produces mesons

FIG. 5 C. Facsimile drawing of a secondary event of the type $2+11_p$ caused by a charged particle in the original shower.

successively losing energy in each step. Such a model might account both for the large spread of the meson showers and for the low excitation produced in the target.

IV. THE NEUTRAL SHOWER PARTICLES

A. *The Ratio of Neutral to Charged Pions*

The ratio of the number of neutral to charged pions has been measured by many observers [Bradt, *et al.* (1950), Carlson, *et al.* (1950), Tinlot and

Gregory (1951), Daniel, *et al.* (1951), Kaplon, *et al.* (1952 A and B), G. Salvini and Y. Kim (1952)]. There is an appreciable discrepancy between values obtained by different observers both at low and at high energies. Since this quantity is of great theoretical interest, additional measurements with modified techniques are desirable. The shower described in the previous section permits a determination which is free from some of the uncertainties of previous measurements, for the following reason:

(1) The ratio of charged mesons to protons is accurately known. Since all particles in the shower have minimum ionization and since they are all confined to a small angular interval the shower must contain all the protons of the projectile (Mg) and the target (O or Si). The number of protons lies therefore between 20 and 26.

(2) The shower passes through 0·7 conversion units (one radiation unit) in the stack and 50% of the conversions take place in the emulsion. It is therefore possible to recognise all the processes which give rise to additional minimum ionization tracks in the shower core and establish what percentage of the increased track number is due to pairs produced by γ-rays, what percentage due to pairs produced by charged particles and what percentage to nuclear interactions of charged and neutral particles.

(3) The number of γ-rays involved is so high that statistical fluctuations do not introduce an appreciable error.

In Fig. 6 we have plotted the observed number of shower tracks in a cone of half angle $5{\cdot}7 \times 10^{-3}$ radians as a function of X, the distance from the origin in conversion units. In the same graph we have plotted the expected increase in track number assuming that the entire increase is due to the conversion of γ-ray pairs from the decay of neutral mesons of varying life times. We have drawn the calculated curves so as to coincide with the experimental values at $X = 0$ and $X = 0{\cdot}178$ by chosing an appropriate value for the number of neutral mesons in the cone. Fig. 6 shows clearly that the experimental points lie on curves for which the meson lifetime in the L-system $\tau \leqslant 10^{-11}$ sec. and the number of neutral mesons nearly equals the number of charged shower particles. The corresponding proper lifetime is $\tau_0 \leqslant 10^{-14}$ sec. Identical results are obtained if we use cones of different aperture. It shows that we can in our experiment neglect effects due to the finite lifetime of the neutral meson. In order to obtain a reliable value for the ratio of neutral to charged mesons, however, a more detailed analysis of the multiplication process is required.

We have surveyed in 17 emulsions the area defined by a shower cone of half angle $1{\cdot}6 \times 10^{-2}$ radians as well as a small additional area near this

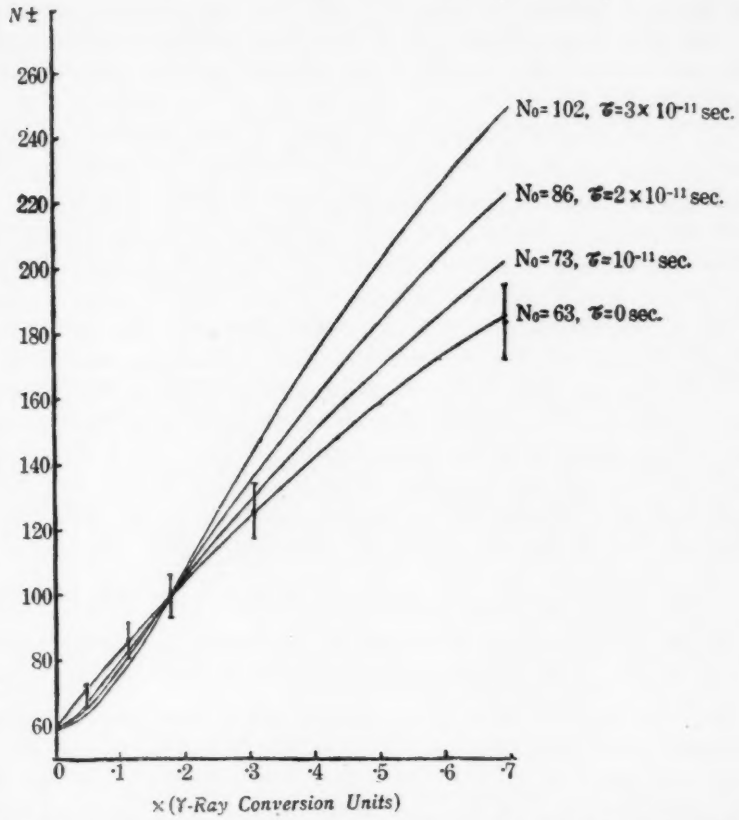

FIG. 6. Number of charged minimum ionizing particles in a cone of aperture $5{\cdot}7\times10^{-3}$ radians as a function of distance from the shower origin. The curves represent the increase calculated for neutral pions of varying lifetimes. The number of neutral pions for each curve is adjusted to give agreement with the experimental point at $X = 0{\cdot}178$.

cone and found the following events in which relativistic particles are produced:

29 High energy pairs produced by γ-rays.

15 High energy pairs produced by charged particles.

56 Shower particles produced in the nine nuclear interactions previously described.

We have determined the number of converted γ-rays and therefore the number of neutral mesons in two ways: the first method which is somewhat

less accurate involves the detection efficiency for γ-ray produced pairs. The second method depends only on the *relative* contribution of the various processes to the total multiplication. Both methods lead to similar results.

(α) Electron pairs are difficult to detect if the origin of the pair lies close to either surface of the emulsion. The efficiency for detecting pairs originating near the centre of the emulsion was assumed to be 100%. Since the origin of pairs must be uniformly distributed in depth throughout the emulsion, we obtain from the length distribution of observed pairs an upper limit on the overall detection efficiency of 75%.

In 17 emulsions and in the area restricted by the cone of $1{\cdot}6 \times 10^{-2}$ radians we observed 24 γ-ray produced pairs. The total number in that area must then be at least 32. Since in each emulsion as well as in each glass backing the track length corresponds to 0·016 conversion units and since the 17 emulsions were nearly equally spaced over a distance from $X = {\cdot}048$ to $X = 0{\cdot}697$ c.u. (comprising 20 nuclear plates) the 32 pairs represent 42% of the numbers of γ-rays converted in this distance. The number of neutral mesons in the cone is therefore given by

$$n_0 = \frac{32}{2 \times 0{\cdot}42}\left(e^{-0.048} - e^{-0.697} \right)^{-1} = 84.*$$

Because of the manner by which the detection efficiency was estimated, the true value may be slightly higher.

At $X = {\cdot}048$ the same cone contains 119 charged shower particles. Correcting for the pairs converted in ·048 c.u., the number of nonelectronic charged particles is 106. Since the entire shower must also contain 20 to 26 protons from the incident (Mg) nucleus and the target (Si or O) nucleus we deduct a corresponding fraction of the total and obtain 93 charged mesons in the cone.

The ratio of neutral to charged mesons becomes

$$\frac{n_0}{n^+ + n^-} = 0{\cdot}9.*$$

(β) We can arrive at the ratio also from the total multiplication of shower tracks.

The contribution to this increase from secondary mesons produced in nuclear collisions is obtained from the angular distribution of shower tracks in the secondary stars. In the angular cone considered, the 9 stars occurring in emulsion contribute 8 tracks. At the same time the seven charged primaries of these stars are eliminated from the cone. Thus the

net increase is only $\frac{1}{9}$ tracks per star. Since the interaction cross-section of charged shower particles was found to be geometric, another 34 similar events must occur in the glass of the plates which will contribute 3·8 tracks to the total increase. After making this small correction the remaining increase of 170 tracks must be attributed to electrons created in 20 emulsions and 20 glass plates inside the cone.

In surveying 17 of these emulsions we find that 19 out of 24 γ-ray produced pairs are completely unresolved in a track length of several hundred microns. Altogether there are among the 48 electrons of these pairs 7 which are emitted under a small angle ($\sim 10^{-2}$) to the direction of the shower particles. These electrons will not contribute to the observed multiplication at the end of the stack since they have comparatively low energy and will be scattered out of the cone which we are considering. Thus only 85% of the γ-ray produced electrons contribute to the multiplication.

The 8 pairs produced by charged particles in the same area have much lower energy. Only 6 of the 16 electrons created are of high enough energy to contribute to the multiplication. Thus of the 170 electrons, 148 come from γ-ray produced pairs and the others from pairs produced by charged particles. In order to obtain 148 electrons $n_\gamma = \dfrac{148}{2 \times 0{\cdot}85} = 87^*$ γ-rays must be converted between 0·048 and 0·697 conversion units. The corresponding number of neutral mesons is $n_0 = 96$ and the ratio

$$\frac{n_0}{n_+ + n_-} = 1{\cdot}0 \pm {\cdot}\,1.^*$$

Within the statistical error this value is in agreement with the value $0{\cdot}71 \pm 0{\cdot}3$ obtained by Kaplon, *et al.* (1952 B) for showers in a similar energy range but without correcting for protons among the charged shower particles. It is however in disagreement with the value $0{\cdot}29 \pm {\cdot}08$ obtained at high energies by Daniel, *et al.* (1951).

We can now correct for the number of pairs converted in ·048 radiation units between the origin of the shower and the first emulsion.

---

* *Note added in proof*: The values marked by asterisks should be reduced by 16% to account for secondary and tertiary pairs created in 0·697 c.u. The calculated corrections have been checked by measuring the multiplication at smaller values of X. Thus we obtain a ratio:

$$\frac{n_0}{n^+ + n^-} = 0{\cdot}86 \pm 0{\cdot}1.$$

We are indebted to Dr. M. F. Kaplon for drawing our attention to this error.

Of the 210 charged shower particles observed (7 mm. from the origin)

22 are electrons from converted γ-rays.

~ 23 are protons.

165 are charged mesons with possibly an admixture of proton-antiproton pairs.

There are also ~ 145 neutral pions, about 23 neutrons and possibly additional neutral particles emitted in the collisions.

The 22 electrons contained in the shower at the point of observation do not introduce an error into the analysis of the angular distribution in Section II. Their inclusion in the analysis is equivalent to including some of the neutral mesons.

B. Cross-Section for the Production of Electron-Positron Pairs by Charged Particles

In the previous section we have analysed the composition of the relativistic particles contained in a cone of half angle $1{\cdot}6 \times 10^{-2}$ radians.

Surveying 17 emulsions we found 15 pairs produced by charged particles of which 8 were lying in the cone. On the basis of an estimated detection efficiency of 75% we believe that the number of such pairs in the surveyed region should be taken to be $10{\cdot}5$. In view of the fact that most γ-ray produced pairs are well separated from the nearest charged particle track we do not believe that an appreciable fraction of pairs attributed to charged particles are in fact coincidences between the track of a charged particle and a pair produced by a γ-ray.

The cone contains the tracks of 106 mesons and protons whose energy in units of their rest masses is of the order of $\gamma_0 \sim 1000$ and a linearly increasing number of electrons with $\gamma_0 \sim 100{,}000$.

The total observed track length in emulsion is 100 cm. or 27 conversion units for mesons and protons and 83 cm. or 22 conversion units for electrons. Using the formulæ given by Bhabha (1935) the cross-section for pair production by singly charged particles in emulsion ($Z_2 \sim 40$) in units of the cross-section for pair production by γ-rays is

$$5{\cdot}6\% \text{ for } \gamma_0 = 10^3$$

$$20{\cdot}5\% \text{ for } \gamma_0 = 10^5.$$

We therefore, expect in the observed region

$1{\cdot}5$ pairs created by mesons or protons and

$4{\cdot}5$ pairs created by electrons,

a total of 6 pairs. These numbers do not critically depend on the assumed values for the energy of the particles. The experimental and theoretical cross sections are therefore found to be in reasonable agreement.

C. *Meson Showers produced by Neutral Shower Particles*

We have observed two meson showers produced by neutral shower particles. Both are of the "jet" type. They are reproduced in Fig. 5.

One shower occurs at a distance of 8·3 cm. from the origin. It has one heavy prong and four well collimated shower particles. It may well have been produced by one of the 20 neutrons which must be present in the primary event.

The second shower is produced at a distance of 4·4 cm. from the origin and located very close to the center of the core. No heavy track and no recoil is associated with this event. It has 5 minimum ionization tracks whose angles with the shower axis are 0·71°, 3·3°, 4·0°, 40·1° and 103° respectively. A star consisting only of minimum ionization tracks diverging at large angles has not previously been observed by us and should be quite rare. In view of the fact that wide emission angles and low number of heavy tracks seem to be characteristic of meson showers produced by charged mesons, it is tempting to attribute the event to the nuclear interaction of a neutral pion. It is easily seen however that the probability of observing such an event at a certain distance from the origin decreases rapidly with the lifetime of the particle. Assuming nuclear geometric cross section, the chance of observing one of the 145 neutral pions in our star to produce a nuclear distintegration in emulsion at a distance of 4·4 or more cm. from the origin is 1% for a lifetime $\tau = 3 \times 10^{-11}$ sec. and 0·05% for a lifetime $\tau = 2 \times 10^{-11}$ sec. Since the energy of a shower particle in the centre of the core is approximately $\gamma_0 \sim 1100\,\mu c^2$, the particle producing the event must have a lifetime in its rest system, $\tau_0 \geqslant 2 \times 10^{-14}$ sec.

In view of the uncertainty in the energy of individual mesons this is not necessarily in contradiction with the lower limit ($\tau_0 \leqslant 10^{-14}$ sec.) obtained in Section IV A, but indicates that the true lifetime must lie very close to this value if the event was produced by a neutral pion. This lifetime is in close agreement with the value obtained previously by a different method (Kaplon, *et al.*, 1952 A).

The secondary interaction on which the lower limit of the lifetime is based, may of course have been produced by different kind of neutral meson of longer lifetime rather than by a neutral pion.

V. CHARGE AND ENERGY BALANCE

According to our analysis, the shower was produced by a primary nucleus of magnesium with energy $1{\cdot}9 \times 10^{14}$ eV incident on a target nucleus of oxygen or silicon. In addition to the original nucleons contained in the shower the collision resulted in the production of 165 charged mesons and an almost equal number of neutral mesons which decay into two γ-rays with a lifetime $\tau_0 \lesssim 10^{-14}$ sec.

The total number of mesons produced at this energy are in agreement with Fermi's theory if we assume that 19 nucleon-nucleon collisions have taken place and that both charged and neutral mesons have a statistical weight of 2.

The nature of the charged shower particles is not known, but if we assume that the γ-ray producing neutral mesons are all neutral *pions*, we get a large excess of neutral over charged pions unless we assume that most of the *charged* shower particles are also pions. If for instance 50% of the charged shower particles were K-mesons or protons and anti-protons the ratio $\frac{n_0}{n_+ + n_-}$ would become nearly equal to 2.

Other neutral mesons of longer lifetime or neutron—anti neutron pairs may also have been produced but in view of the fact that 8 out of 10 secondary nuclear interactions were initiated by charged particles this number of longlived neutral particles, if they are produced, is likely to be much smaller than the number of charged shower particles.

From the point of view of charge symmetry the simplest and most satisfactory assumption would be that all the mesons are pions. A consideration of the energy balance of the collision neither confirms nor contradicts this view.

An energy balance for the total event can be established only very roughly since the number of nucleon-nucleon collisions contributing to the shower is not known. In view of the absence of heavy fragments from the incident nucleus we shall assume that at least 12 of the incident nucleons were involved in the collision. In each interaction an energy of 130 MC^2 is available in the C-system. Thus we have to account for at least 1560 MC^2 in terms of mesons and nucleons if complete inelasticity is assumed. We have obtained an energy of $8{\cdot}4\,\mu c^2$ for the mesons in the C-system. If we assume that all of them are pions they will account for only 400 MC^2. The 24 nucleons assumed to be involved in the collision will account for not more than 200 MC^2. This leaves 60% of the available energy unaccounted for.

It seems difficult to remove this discrepancy by drastically reducing the energy of the incident nucleus or raising that of the average meson produced because the *ratio* of nucleon to meson energy in the C-system is completely determined by the maximum spread of the shower which in our case seems to be well defined. This discrepancy is reduced if we assume that many of the shower particles are much heavier than pions but another plausible explanation is suggested by the observations of Kaplon, *et al.* (1952 A) on the T-shower. Here two of the 17 neutral mesons carry 62% of the entire energy appearing in the soft component. Observations which lend themselves to a similar interpretation were reported by Hopper, *et al.* (1951). In view of the evidence that a large fraction of the energy may be concentrated in a small number of shower particles, we feel that the energy balance of showers cannot safely be used to arrive at conclusions about the mass of shower particles.

The energy of $1{\cdot}9 \times 10^{14}$ eV for the incident nucleus is the highest as yet observed in the heavy component of primary radiation. It suggests that the constancy of the chemical composition of primary radiation which has been shown to hold certainly up to energies of 10^{11} eV/nucleon (Lal, *et al.*, 1952) may in fact extend to the highest energies appearing in cosmic radiation. If this assumption is correct, then events like the large Auger showers whose detection depends on the total energy of the primary rather than on its energy per nucleon will mainly be initiated by very heavy nuclei.

VI. Conclusions

The angular distribution of shower particles in showers produced by nuclei, will for very high multiplicities determine the energy of the primary as well as the energy of the secondary particles, if most of the latter are assumed to be reasonably monoenergetic in the C-system. For a shower containing nearly 200 charged shower particles produced by a Magnesium nucleus of $1{\cdot}9 \times 10^{14}$ eV, the angular distribution agrees closely with the predictions of Fermi's theory. The observed multiplicity at this energy is also consistent with the theory.

The charged shower particles interact with geometric cross-section and (at energies of the order of $1000\,\mu c^2$) produce secondary showers with an average multiplicity $n_s = 5$ to 6. The secondary showers are characterised by a very wide angular spread and a low number of slow fragments indicating small excitation of the target nucleus. The mesons in meson produced showers are preferentially emitted in the backward direction.

The charged shower particles of the main event do not arise from a shortlived heavy parent meson.

Charged shower particles as well as electrons produce electron pairs with a cross-section which is close to the cross-section derived by Bhabha.

The number of neutral pions decaying into γ-rays in a time less than $\sim 10^{-14}$ sec. is very nearly equal to the number of charged shower particles produced.

There is evidence for the emission of neutral interacting particles different from neutrons. If these particles are neutral pions their lifetime must be *equal* to 10^{-14} sec. within a factor of two. If they are not pions but particles of longer lifetime their number is considerably smaller than the number of charged shower particles or neutral pions.

Charge symmetry suggests that nearly all the charged shower particles are pions. Considerations of the energy balance in the collision suggest that a few shower particles carry an appreciable fraction of the total energy.

VII. ACKNOWLEDGEMENT

We are greatly indebted to Mr. P. N. Krishnamurthy and to Mr. Vijayaraghavan for assistance in scanning and preparing graphs and particularly to Dr. H. J. Bhabha for many valuable discussions.

VIII. REFERENCES

1. H. J. Bhabha .. *Proc. Roy. Soc.*, 1935, **152 A**, 559.
2. H. L. Bradt, M. F. Kaplon, B. Peters .. *Helvetica Physica Acta*, 1950, **23**, 24.
3. Camerini, Fowler, Heitler, King and Powell .. *Phil. Mag.*, 1949, **40**, 862.
4. Carlson, Hooper and King .. *Ibid.*, 1950, **41**, 701.
5. R. R. Daniel, J. H. Davies, J. A. Mulvey and D. H. Perkins .. (Bristol Conference, 1951).
6. M. Danysz, W. O. Lock, G. Yekutieli .. *Nature*, 1952, **169**, 365.
7. E. Fermi .. *Phys. Rev.*, 1951, **81**, 683.
8. V. D. Hopper, S. Biswas, J. F. Darby .. *Ibid.*, 1951, **84**, 457.
9. M. F. Kaplon, B. Peters and D. M. Ritson .. *Ibid.*, 1952 **A**, **85**, 900.
10. M. F. Kaplon and D. M. Ritson .. *Ibid.*, 1952 **B**, **85**, 932.
11. D. Lal, Yash Pal, M. F. Kaplon and B. Peters .. *Ibid.*, 1952, **86**, 569.
12. G. Salvini and Y. Kim .. *Ibid.*, 1952, **85**, 921.
13. J. Tinlot and B. Gregory .. *Ibid.*, 1951, **81**, 667, 675.

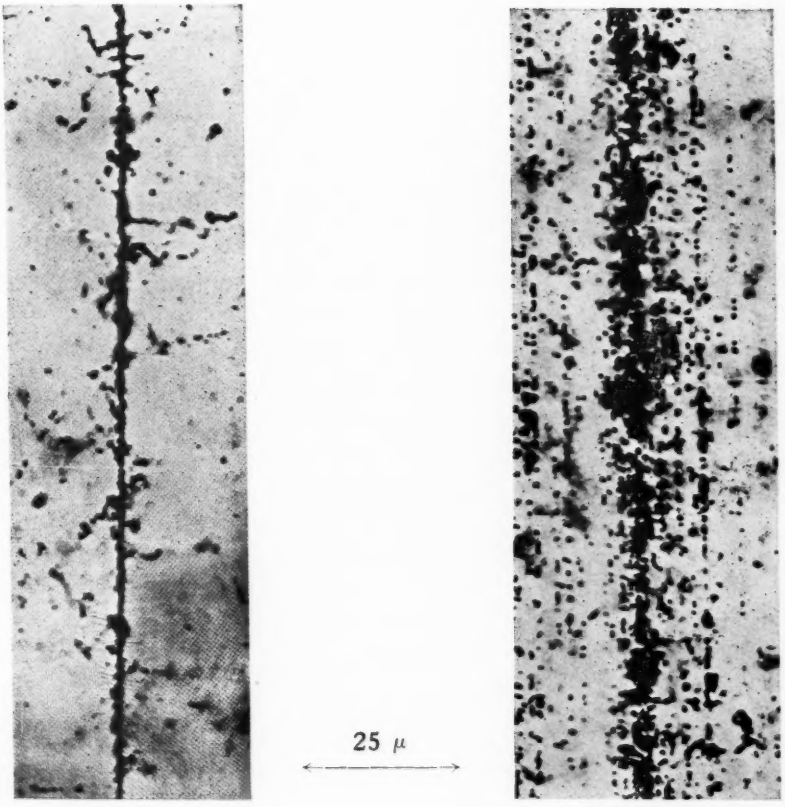

FIG. 1. Shows the track of a Magnesium Nucleus which causes a shower of 210 charged particles. Part of the shower core at a distance of 5·1 mm. from the origin is shown on the right.

COSMIC RAYS UNDERGROUND

By B. V. Srikantan and S. Naranan
(*Tata Institute of Fundamental Research, Bombay-1*)

Received May 12, 1952
(Communicated by Prof. H. J. Bhabha, F.A.SC., F.R.S.)

During the months of October, November and December, 1951, an investigation on cosmic-ray intensity was carried out in the Gold Mines at Kolar (Mysore State) surface altitude 2,800 ft., with a hodoscoped counter telescope, upto a depth of 1,008 meters water equivalent. The experimental details, and the main results of the investigation are presented in this paper under the following Sections:—

Section I. Experimental details.
Section II. Intensity Measurements, vertical flux at various depths.
Section III. Angular Distribution of underground particles.
Section IV. Production of Secondaries by μ-mesons.
Section V. Deduction of the Energy Spectrum of π-mesons and of μ-mesons from the intensity measurements.
Section VI. Nature of the neutral radiation underground.
Section VII. Comparison of results with the results of other experiments and Discussion.

Section I. Experimental Details

The apparatus used is shown in Fig. 1. Six counters of length 37·5 cm. and diameter 4·0 cm. were placed in each of the trays A, B, C and D. The trays A and B were separated by a lead absorber 2·5 cm.

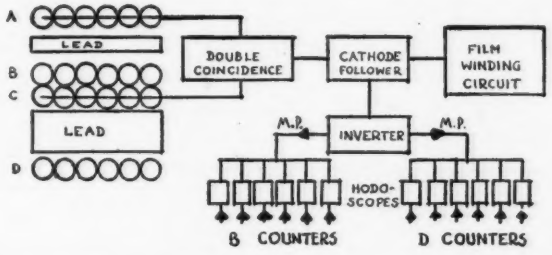

Fig. 1. Block Diagram Showing the Essential Electronic Circuits.

thick, and trays C and D by a lead absorber 7·5 cm. thick. The extreme trays A and D were separated by 27·5 cms. The semi-angles of acceptance of the telescope ABCD were 40° and 54° in the planes perpendicular and parallel to the counter axes. The semi-angles of ABC in the two planes were 60° and 68°. All the counters were filled with argon and petroleum ether in the ratio 9 : 1, to a total pressure of 10 cm. The counters were operated about 50 volts above the threshold voltage. The efficiency of the counters was found to be 98·5%.

The counters in trays B and D were hodoscoped with AC double coincidence pulse as the master triggering pulse.* A block-diagram showing the essential electronic circuits is given in Fig. 1. The circuit diagrams of the hodoscope and the film-winding circuit are given in Fig. 2 (*a*) and Fig. 2 (*b*). Each hodoscope plug-in unit consisted of a twin-triode (7F7)

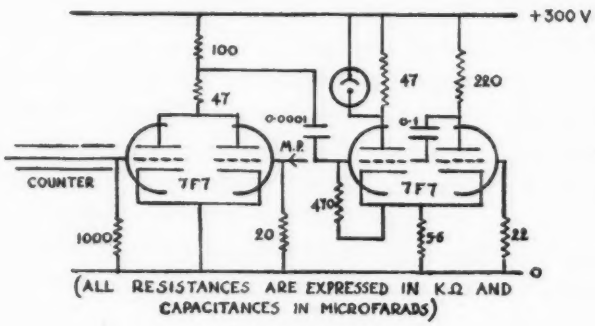

FIG. 2 (*a*). Hodoscope Circuit.

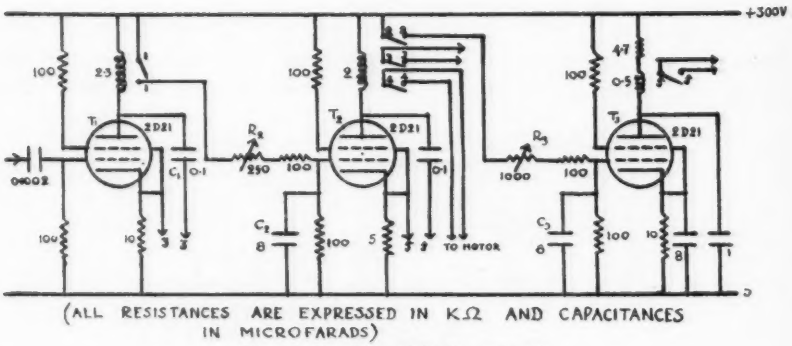

FIG. 2 (*b*). Film Winding Circuit.

* At 10 and 22 mwe, where the AC rate was too high for photography every thirty-second AC pulse was taken as the master pulse.

which selected coincidences of the AC master pulse, and the counter pulse; and a univibrator (7F7) to broaden the coincidence pulse for flashing a neon indicator. Since the plug-in units were placed close to the counter trays, it was not found necessary to use a pre-amplifier-cathode-follower-inverter system for every counter. For AC double coincidence, 6AK5 miniature pentodes were used. The coincidence pulse was fed to a 6J6 cathode-follower. Two outputs were taken from the cathode point of the cathode-follower. One output, after inversion, served as the master-pulse for all the coincidence stages of the hodoscopes. The second output was fed to the grid of the first thyratron of the film winding circuit.

Since the neon indicators connected in the plate of the univibrators flashed for a considerable time, it was essential to introduce a delay between the arrival of the master pulse on the grid of the first thyratron and the winding of the film. This was achieved by the thyratron delay circuit shown in Fig. 2, in the following way: With the arrival of the master pulse, the thyratron T_1 fired. It was not switched off immediately since the condenser C_1 was not connected to the cathode. A pair of off-to-on contacts of the relay in the plate of T_1 began charging the condenser C_2 in the grid of T_2 through the resistance R_2. As soon as the voltage on C_2 rose above the cut-off bias of T_2, the thyratron T_2 fired. T_2 too was not switched off immediately. The relay in the plate of T_2 had three pairs of off-to-on contacts. One pair switched off T_1 by connecting C_1 to the cathode of T_1. Another pair put on the D.C. voltage for the film-winding motor. The third pair started charging C_3 through R_3. As soon as the voltage on C_3 exceeded the cut-off bias of T_3, the thyratron fired, but was automatically switched off. The pair of contacts of the relay in the plate of T_3 switched off T_2. The delay time was controlled by C_2 and the potentiometer R_2, and the winding time of the motor by C_3 and the potentiometer R_3.

The experiment was first carried out at the surface. Then it was repeated at depths 503, 598, 807, 1008 mwe. The 22 mwe level was covered at the end. Though the main shaft was very wet, the places at which the experiment was set up, were comparatively free from moisture. Except at 1008 and 22 mwe, the telescope was more than 600 ft. away from the main shaft, at all depths. At 1008 mwe, it was 200 ft. away and at 22 mwe, about 10 ft. away from the shaft.

Section II. Intensity Measurements

From the hodoscope photographs, we were able to deduce the following counting rates:—

(i) the three-fold coincidence rate N_{ABC} (counts per hour) of particles capable of penetrating 2·5 cm. of lead, recorded by the telescope with semi-angles of acceptance 60° and 68° in the two planes;

(ii) the four-fold coincidence rate N_{ABCD} (counts per hour) of particles penetrating 10 cm. of lead, recorded by the telescope with semi-angles 40° and 54°;

(iii) the four-fold coincidence rate of particles penetrating 10 cm. lead, as recorded by a system of five single counter telescopes with semi-angles 12° and 64°.

Table I gives the recorded rates N_{ABC}, N_{ABCD} at various depths. They are plotted against depth expressed in mwe on a log-log scale in Fig. 3. The

TABLE I

Depth H mwe	$E_{min.}$(Bev) of μ-mesons penetrating H mwe	N_{ABC} (counts per hr.)	N_{ABCD} (counts per hr.)	I_{ABC}	I_{ABCD}	I_v	$\frac{I_{ABCD}}{I_{ABC}} \times 100$
10	2·966	21440±610	9414±410	$7{\cdot}42 \times 10^{-3}$	$5{\cdot}88 \times 10^{-3}$	$6{\cdot}11 \times 10^{-3} \pm 0{\cdot}49 \times 10^{-3}$	79·2
22	6·425	9215±272	3806±173	$3{\cdot}71 \times 10^{-3}$	$2{\cdot}67 \times 10^{-3}$	$2{\cdot}87 \times 10^{-3} \pm 0{\cdot}23 \times 10^{-3}$	72·0
503	152·8	54·3±2·6	25·6 ±1·8	$2{\cdot}56 \times 10^{-5}$	$2{\cdot}04 \times 10^{-5}$	$1{\cdot}76 \times 10^{-5} \pm 0{\cdot}24 \times 10^{-5}$	79·7
598	186·6	30·8±1·3	14·7 ±0·9	$1{\cdot}46 \times 10^{-5}$	$1{\cdot}19 \times 10^{-5}$	$1{\cdot}24 \times 10^{-5} \pm 0{\cdot}13 \times 10^{-5}$	81·5
807	269·5	11·4±0·6	5·3 ±0·4	$0{\cdot}539 \times 10^{-5}$	$0{\cdot}425 \times 10^{-5}$	$0{\cdot}555 \times 10^{-5} \pm 0{\cdot}070 \times 10^{-5}$	78·8
1008	370·6	4·74±0·21	2·33±0·15	$0{\cdot}224 \times 10^{-5}$	$0{\cdot}187 \times 10^{-5}$	$0{\cdot}237 \times 10^{-5} \pm 0{\cdot}027 \times 10^{-5}$	83·5

(The intensities I_{ABC}, I_{ABCD}, and I_v expressed in terms of particles cm.$^{-2}$ sec.$^{-1}$ sterad^{-1} have been computed using $\cos^3$ angular distribution for 10 mwe, $\cos^3$ distribution for 22 mwe, and $\cos^4$ distribution for 503–1008 mwe.)

last four experimental points corresponding to particles capable of penetrating 10 cm. lead, can be fitted to the straight line

$$\log_{10} N_{ABCD} = 10{\cdot}62 - 3{\cdot}41 \log_{10} H.$$

Similarly, the last four N_{ABC} rates, can be fitted to the straight line

$$\log_{10} N_{ABC} = 11{\cdot}30 - 3{\cdot}55 \log_{10} H.$$

These lead to the intensity-depth relations

$$N_{ABCD} = 10^{10{\cdot}62} H^{-3{\cdot}41 \pm 0{\cdot}01} \quad (1)$$

$$N_{ABC} = 10^{11{\cdot}30} H^{-3{\cdot}55 \pm 0{\cdot}06} \quad (2)$$

For the component penetrating 10 cm. of lead the slope of the line joining the surface point to the 22 mwe point is 1·15, and the corresponding

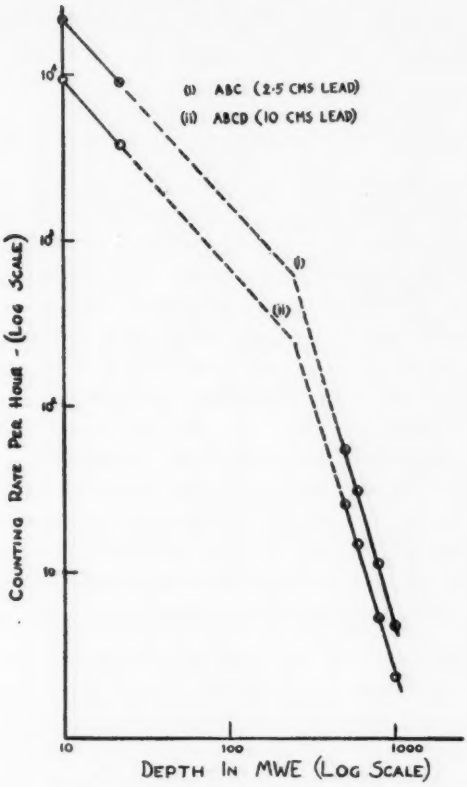

FIG. 3. Counting Rate—Depth Curves.

slope for radiation penetrating 2·5 cm. lead is 1·09. It is seen that for depths below 503 mwe, the absorption curves for the particles penetrating 2·5 and 10 cm. lead, run almost parallel. From the last column of Table I, it is seen that at all depths, nearly 80% of the particles penetrating 2·5 cm. lead are capable of penetrating 10 cm. lead.

Table I gives the flux values I_{ABC}, I_{ABCD}, and I_V, calculated from ABC, ABCD and the single-counter telescope counting rates, and also the ratio I_{ABCD}/I_{ABC}. The computations were made assuming $\cos^2$ angular distribution at 10 mwe, $\cos^3$ distribution at 22 mwe and $\cos^4$ distribution for depths 503–1008 mwe. The reasons for choosing these cosine powers are discussed in the following section (III). In the calculation of vertical flux, the angular distribution in both the planes was taken into account. The vertical flux I_V calculated from the single counter telescopes is more

accurate, since the effect of leakage spaces is a minimum. Between 500 and 1008 mwe the vertical intensities can be expressed by the power law,

$$I_V = 10^{3.56} H^{-3.1 \pm 0.1} \quad (3)$$

SECTION III. ANGULAR DISTRIBUTION OF UNDERGROUND PARTICLES

A detailed description of the procedure adopted for obtaining the angular distribution of underground particles, from the hodoscope records is given in the Appendix. The results are given in Fig. 4 and Fig. 5. The solid lines in the figures represent the distributions expected on the basis of $\cos^2$, $\cos^3$, and $\cos^4$ laws. The experimental points for the four angles 0°, 15½°, 29°, and 40° are also plotted in the same figures for the two depths 22 mwe and 598 mwe. It is seen that at 22 mwe, the experimental points are closer to the $\cos^3$ curve rather than $\cos^2$ or $\cos^4$ curves. But at 598 mwe, the experimental points are closer to the $\cos^4$ curve. While the number of particles recorded, particularly at large inclinations, is not sufficiently high for deciding unambiguously on the exact power law obeyed, the increasing steepness of the angular distribution curve with depth is unmistakable. However, it may be pointed out that in the computation of vertical flux, a change from $\cos^2$ to $\cos^3$ distribution increases the calculated flux by only 5%. The corresponding increase, when the distribution changes from $\cos^3$ to $\cos^4$ is 7%.

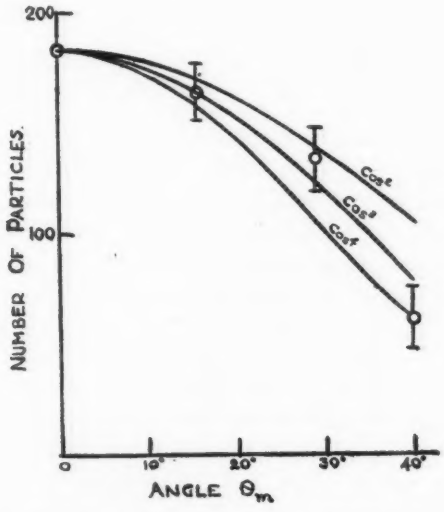

FIG. 4. Angular Distribution at 22 Mwe.

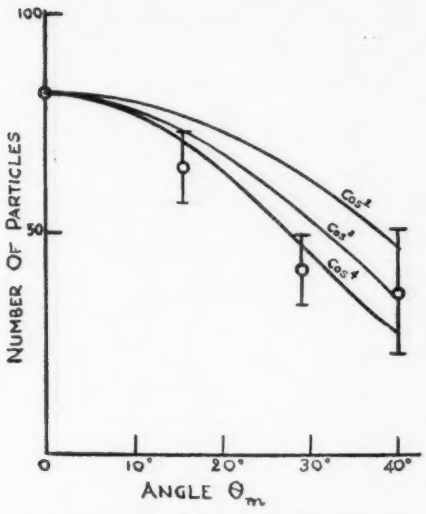

FIG. 5. Angular Distribution at 598 Mwe.

SECTION IV. PRODUCTION OF SECONDARIES BY μ-MESONS

(*A*) *Secondary production in the lead of the apparatus*

The experimental arrangement used for the measurement of intensity was suitable also for finding the percentage of μ-mesons that produced secondaries such as knock-on's, bremsstrahlung electrons, etc., in the lead of the apparatus. For this purpose, the ABCD hodoscope events were classified into two groups: (1) Events with one discharged counter in tray B, and one discharged counter in tray D ($B = 1$, $D = 1$). (2) Events with more than one counter discharged in either B or D, or in both. The events of the second group, which we shall call 'multiple events' can be classified according to the number of counters triggered in trays B and D. Table II gives a full and detailed analysis of the multiple events at various depths. All the multiple events can however be divided into three main categories:—

(i) one counter discharged in tray B and more than one counter discharged in tray D ($B = 1$, $D > 1$)

(ii) more than one counter discharged in tray B and one counter discharged in tray D ($B > 1$, $D = 1$)

(iii) more than one counter discharged in tray B and more than one counter discharged in tray D ($B > 1$, $D > 1$)

TABLE II

Complete and detailed analysis of the multiple events at various depths

Depth mwe	B=1, D=1 Singles	B=1, D=2					B=1, D=3			B=1, D=4	B=1, D=5	B=1, D=6	B=2, D=1					B=3, D=1				B=4, D=1	B=6, D=1	B=2, D=2	B=3, D=2	B=4, D=2	B=6, D=2	B=2, D=3	B=4, D=3	B=6, D=3	B=2, D=4	B=5, D=4	B=4, D=5	ABCD
		q = 0	1	2	3	4	Total	q = 0	1	Total				q = 0	1	2	3	4	Total	q = 0	1	2	Total												
10	503	11	2				13	1		1				18	2	1			21		2		2	1												541
22	449	7	1				8	1		1	1			9	3	1			13	1			1			1									474
503	167	12	2	1			15				1			14	1	3			18	2	1		3	1		1	1	1							208
598	236	17		1			18	3	1	4				15	2	1			18	5			5	1		1						2		2	287
807	156	13					13	5	1	6				9		1			10	2			2			2			2						191
1008	193	11	2			1	14	4		4	3	2	1	14	1				15	8	2		10	3	3	2	1		2	2	2	1	1		259

q stands for the number of undischarged counters intervening the discharged counters.

Table III gives the observed number of events falling into each of the various categories described above, and also the percentage values to facilitate comparison.

TABLE III

Classification of the hodoscope records, Arrangement I

Event \ Depth mwe	10 mwe	22 mwe	503 mwe	598 mwe	807 mwe	1008 mwe
ABCD	541	474	208	287	191	259
B=1, D=1	503 93·0±4·1	449 94·7±4·5	167 80·3±6·2	236 82·3±5·4	156 81·7±6·5	193 74·5±5·4
B=1, D>1	14 2·6	10 2·1	16 7·7	22 7·7	19 10·0	24 9·3
B>1, D=1	24 4·4	14 3·0	22 10·6	24 8·4	12 6·3	31 12·0
B>1, D>1	0 0	1 0·2	3 1·4	5 1·6	4 2·0	11 4·2
Multiple Events	38 7·0±1·1	25 5·3±1·3	41 19·7±3·1	51 17·7±2·5	35 18·3±3·1	66 25·5±3·1

Interpretation of the events

In the interpretation given below, the effect of the dead-space leakages of the counter geometry have been neglected. We assume that the leakage factor is the same at all depths, and regard the estimated percentages of multiple events as useful only for comparing the values at different depths.

1. *Events of the type* $B = 1$, $D = 1$.—These events are mostly due to:

   (*a*) single particles penetrating 10 cm. lead without producing secondaries;

   (*b*) single particles producing secondaries that pass through the same counters as the single particles;

   (*c*) two or more closely collimated penetrating particles passing through the same counters in B and D.

Without an exact knowledge of the angular distribution of the secondary particles, it is not possible to separate the contributions from the various groups. By regarding all the events of type $B = 1$, $D = 1$, as single particles, we obtain an upper limit to the number of single particles and a corresponding lower limit to the number of particles that are accompanied by secondaries.

2. (i) *Events of type* $B = 1$, $D > 1$.—Events of this type are caused by

(*a*) single penetrating particles producing secondaries in the 7·5 cm. lead between the trays C and D, the angles of emisison of the secondaries being sufficiently large for the secondaries, or the showers initiated by them to trigger neighbouring counters;

(*b*) two or more penetrating particles with angular separation such that they pass through the same counters in B and through different counters in D.

It is again difficult to separate the relative contributions of (*a*) and (*b*). Since it was observed that the events in which two neighbouring counters were discharged in both B and D were few [(in type (iii)], the contribution from the second type may be considered small compared to that from the first type (*a*). It is seen from Table III, that the percentage of these events increases from 2·6% at 10 mwe to 9·3% at 1008 mwe.

(ii) *Events of type* $B > 1$, $D = 1$.—These events are due to

(*a*) single penetrating particles incident on the telescope, accompanied by secondaries that can penetrate 2·5 cm. lead;

(*b*) single penetarting particles producing secondaries in 2·5 cm. lead plate, that cannot penetrate 7·5 cm. lead.

The upper limit to the contribution from the first type of events (*a*) was determined from a modified experimental arrangement (Arrangement II, as distinguished from the set-up of Fig. 1, which is Arrangement I) described in sub-section (B). From this, the lower limit to the percentage of particles that produced secondaries in the 2·5 cm. lead plate was known. Table IV gives the lower limits of percentages of secondaries produced in 2·5 cm. and in 7·5 cm. lead, for the three depths 22, 598 and 1008 mwe.

(iii) *Events of type* $B > 1$, $D > 1$.—These events are due to

(*a*) associated penetrating particles arriving from the rock;

(*b*) single particles producing penetrating secondaries in 2·5 cms. lead, with large angular separation;

(*c*) single particles producing secondaries in both the lead plates—double knock-on's, etc.

The total number of observed events of this type were small. The percentage increased from 0·2% at 22 mwe, to 4·5% at 1008 mwe.

TABLE IV

Secondary production in the lead of the apparatus and the rock

Description of event \ Depth (mwe)	10	22	503	598	807	1008
Percentage of particles which produce secondaries in 7·5 cm. lead block in the apparatus (lower limits)	2·6	2·1	7·7	7·7	10·0	9·3
Percentage of particles which produce secondaries in 2·5 cm. lead in the apparatus (lower limits)		2·8		5·8		8·9
Percentage of particles which produce secondaries in the lead of the apparatus (lower limits)		4·9		13·5		18·2
Percentage of events with particles coming as multiples from the rock, corrected (lower limits)		8·4		42·9		41·0

(*B*) *Secondary production in the rock*

To determine the percentage of particles that arrived at the telescope, accompanied by secondaries produced in the rock, the following modification was made in the experimental arrangement: The tray D which was below the 7·5 cm. lead block, was now placed above the tray A. The rest of the set-up remained the same. The counters in trays D and B were hodoscoped as before, with AC double coincidence pulse as the master pulse.

As in sub-section (A), the events were classified as follows:—

(i) *Events of type* $D = 1$, $B = 1$.—These events are due to

(*a*) single particles penetrating 2·5 cm. lead;

(*b*) closely collimated associated particles passing through the same counters in D and B;

(*c*) single particles producing secondaries in the 2·5 cm. lead plate, the secondaries passing through the same counter in D, as the primary.

By regarding all the events $D = 1$, $B = 1$, as due to single particles, we obtain a lower limit for the number of events with associated particles arriving from the rock. The percentage of the events $D = 1$, $B = 1$, decreases from 89% at 22 mwe, to 59% at 1008 mwe (Table V).

(ii) *Events of type* $D = 1$, $B > 1$.—These are due to

(*a*) single particles penetrating 2·5 cm. lead, producing secondaries that trigger the neighbouring counters in tray B;

(*b*) penetrating particles from the rock, which pass through the same counter in D, and through different counters in B.

It is seen from Table V, that the percentage of these events does not change appreciably with depth. These events could be caused by mesons as well as penetrating electrons.

TABLE V

Classification of the hodoscope events of Arrangement II

Event \ Level	22 mwe	598 mwe	1008 mwe
DABC	548	310	203
D=1 } B=1 }	485 88·5±4·0	184 59·4±4·4	120 59·1±5·4
D=1 } B>1 }	33 6·0±1·1	29 9·4±1·8	16 7·9±2·0
D>1 } B=1 }	28 5·1±1·0	84 26·9±2·9	52 25·6±3·6
D>1 } B>1 }	2 0·4	13 4·3±1·2	15 7·4±1·9
Events with particles coming as multiples from top (D>1, B≧1)	30 5·5	97 31·2±3·2	67 33·0±4·0

(iii) *Events of type* $D > 1$, $B \geq 1$.—These events are due to particles which arrive as multiples from the rock. In this case, it was possible to get an estimate of the percentage of particles which were associated with secondaries that passed through the same counter as the primary particle. The calculation was made assuming a Gaussian distribution for the separation of particles, since the separation is governed mostly by scattering. From the frequency of events as a function of separation of the discharged counters, we calculated the constants of the distribution, and were able to get an estimate of the percentage of events in which closely collimated particles passed through the same counter. The corrected percentages of particles that arrived at the telescope as multiples for the three depths 22, 598 and 1008 mwe, are given in Table IV. It is found that

the percentage increases from 8% at 22 mwe to 42% at 1008 mwe. Comparison of these values with theoretical values is given in Section VII (C).

The events of the type $D > 1$, $B > 1$, in Arrangement II, were useful in finding the lower limit to the number of cases in which single penetrating particles produced secondaries in 2·5 cm. lead of the experimental arrangement I. Events of the type $D > 1$, $B > 1$, were those in which two or more particles came from the rock, each capable of penetrating 2·5 cm. lead, or one or both of them produced showers that triggered more than one counter in B. Therefore by regarding all events of the type $D > 1$, $B > 1$, as those in which two or more particles arrived from rock, with at least one of them capable of penetrating 10 cm. lead, we obtain an upper limit to the percentage of such events. This sets the lower limit to the percentage of cases in which secondaries were produced in the 2·5 cms. lead plate of arrangement I.

Section V. Deduction of the Energy Spectrum of π-Mesons and of μ-Mesons from Intensity Measurements Underground

If we make the assumption that μ-mesons are produced only as a result of the decay of π-mesons, then we normally expect the spectrum of μ-mesons to follow closely the energy spectrum of π-mesons at all energies, since the mass difference between π's and μ's is small. But at high energies the probability of absorption of π-mesons increases relative to the decay probability. This renders the μ-meson spectrum at the high energy end steeper than the spectrum of π-mesons in the corresponding energy range. If the differential energy spectrum of π-mesons at production is given by the power law $dN_\pi(E) = k \cdot E^{-r} dE$, and if we assume that the cross-section for the absorption of π-mesons is nuclear geometric upto the energies considered, then the μ-meson differential spectrum is given by (George, 1952; Greisen, 1948)

$$dN_\mu(E) = \frac{k \cdot E^{-r}}{1 + aE} \cdot dE$$

where $\frac{1}{a} = \frac{8 \times 10^5 \cdot m_\pi}{c\tau_\pi}$, m_π = rest energy of π-meson in Bev = 0·143 and τ_π = mean life-time of π-meson = $2 \cdot 4 \times 10^{-8}$ sec., and E is expressed in Bev. When π-mesons decay into μ-mesons the average energy of the μ-mesons is about 0·81 times the energy of the π-mesons. The integral energy spectrum of μ-mesons is therefore given by

$$N_\mu\ (> 0 \cdot 81\, E) = \int_E^\infty \frac{k \cdot E^{-r}}{1 + aE} \cdot dE \qquad (4)$$

To compare the experimentally determined intensities at various depths with the energy spectrum (4), we need the range-energy relation of μ-mesons. The range-energy relation of μ-mesons, considering the energy losses due to ionisation, bremsstrahlung, production of electron pairs, stars, penetrating particles, and Cerenkov radiation is given by (George, 1952)

$$R = \frac{2\cdot303\times10^{-2}}{b}\log_{10}\left(1+\frac{bE}{d}\right), \tag{5}$$

where R and E are expressed in mwe and mev respectively. The constants b and d are determined by the mean atomic number Z and the mean atomic weight A of the material traversed. From the chemical composition of the rock underground (Hornblend Schist, sp.gr. 2·98), the mean value $Z = 11$, and $A = 22$, have been computed. These lead to the values $b = 5\cdot36\times10^{-6}$ gm.$^{-1}$cm.$^{+2}$, and $d = 2\cdot65$ Mev gm.$^{-1}$cm.$^{+2}$. From (5), the minimum energies of μ-mesons penetrating the various depths are calculated and given in Table I (column 2). The depths between 500 and 1008 mwe, roughly correspond to minimum μ-meson energies E_{min} between 150 and 400 Bev. The μ-meson integral spectrum (4) has been drawn in Fig. 6 on log-log scale (for the energy range $150 < E < 400$ Bev), for various

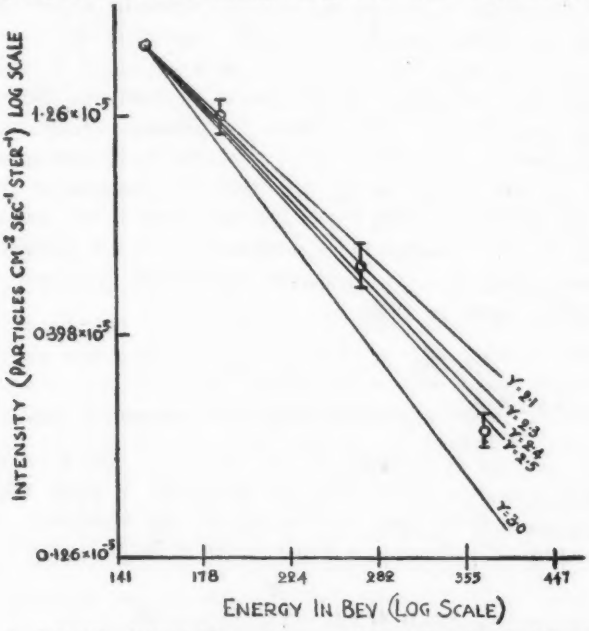

FIG. 6. Integral μ-Meson Energy Spectrum ($150 < E < 400$ Bev) for various values of γ—the exponent of the π-Meson Differential Spectrum.

values of γ, the exponent in the differential energy spectrum of π-mesons. Integration of (4) for non-integral values of γ is performed graphically. In the same figure, the experimental points obtained by us are also plotted. The curves have been normalised with respect to the 153 Bev experimental point (503 mwe). It is observed that the curves drawn with γ between 2·3 and 2·5 agree better than those with $\gamma = 2{\cdot}1$, or 3·0. The curve with $\gamma = 3{\cdot}0$ is much too steep and the one with $\gamma = 2{\cdot}1$ is much too flat to account for the observed experimental intensities. Therefore, a π-meson differential spectrum with the value of the exponent in the neighbourhood of 2·4, in the energy range $200 < E < 450$ Bev, fits best with our experimental results.

It is seen from Fig. 6, that the curves are not very different from straight lines. This means, that in the energy range under consideration ($150 < E < 400$ Bev), the integral spectrum of μ-mesons can be represented by a power law of the form $N_\mu (> E) = \text{constant}.\ E^{-\gamma}$. A least square fit for the first three experimental points gives the straight line

$$\log_{10} N_\mu (> E) = -0{\cdot}178 - 2{\cdot}09 \log_{10} E,$$

where N, the vertical flux is expressed in particles $cm.^{-2}sec.^{-1}sterad^{-1}$. This yields the power law for μ-meson integral spectrum

$$N_\mu (> E) = 0{\cdot}664\ E^{-2{\cdot}09 \pm 0{\cdot}02} \qquad (6)$$

in the energy range $150 < E < 300$ Bev. The least square fit for all the four points yields an exponent 2·41 instead of 2·09.

Section VI. Nature of Neutral Radiation Underground

The counting rates of the trays A, B, C and D, decreased by a factor five from 10 mwe, to 503 mwe, and remained practically the same at all lower depths. Coincidence experiments revealed that the contribution of charged particles to the tray counts was negligible, compared to that of the neutral radiation, converted in the counter walls. The efficiency of the counters for the detection of neutral radiation was obtained by determining the counting rate of a single counter, and the double coincidence rate of the single counter and a system of concentric ring of counters. The measured efficiency was about 1% and was the same as the efficiency of the counters for gamma rays, measured with a gamma source. The counting rate of a single counter was reduced only by 60% when it was shielded on all sides by 2·5 cm. lead. The energy of the gamma rays should be 2·5 mev, if 40% of the rays should be capable of penetrating 2·5 cm. lead. The radiation was found to be isotropic. The neutral radiation in the mines, is therefore essentially of radioactive origin.

SECTION VII. COMPARISON OF THE RESULTS WITH THE RESULTS OF OTHER EXPERIMENTS AND DISCUSSION

(*A*) *Intensity of cosmic rays at various depths*

Intensity measurements have been carried out previously by Wilson (1938) upto a depth of 1406 mwe, and by Clay and Gemert (1939) upto a depth of 1107 mwe. Wilson measured the total intensity with a four-fold coincidence single counter telescope, without any absorber between the counters. Clay and Gemert measured the intensity of penetrating radiation with a four-fold coincidence telescope of semi-angles 35° and 63°, and 10 cm. lead in the telescope. Total intensity was also measured by Miesowicz, *et al.* (1950), at depths 540 and 660 mwe. Miyazaki (1949), in Japan, measured the intensity of penetrating particles at depths 1400 and 3000 mwe. In order to compare our intensity measurements with those the above workers, we have calculated the vertical flux in terms of particles $cm.^{-2}\,sec.^{-1}\,sterad^{-1}$ from the counting rates given by the various workers, assuming a $\cos^4$ angular distribution for the particles at depths below 400 mwe. The calculated flux values of various workers are plotted in Fig. 7.

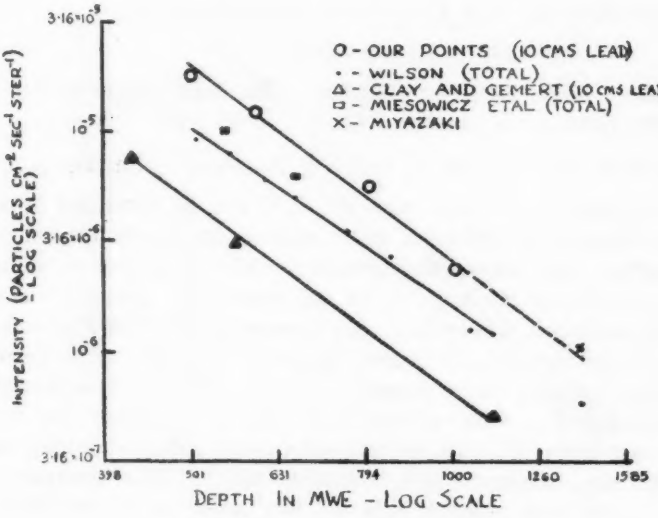

FIG. 7. Comparison of flux values of different workers.

It is seen that at all depths our flux values for the penetrating component are higher than the total intensity values of Wilson and Miesowicz,

et al., by a factor 2. Again our intensities for penetrating particles are higher than the corresponding intensities of Clay and Gemert by a factor 4·5. The flux value of Miyazaki for penetrating particles at 1400 mwe is twice the value of Wilson for total intensity at 1406 mwe. Extrapolating our curve to 1400 mwe shows that Miyazaki's flux value is consistent with our flux values obtained for depths 500–1008 mwe.

(*B*) *Angular distribution of particles underground*

Our measurements of the angular distribution give a $\cos^3$ variation at 22 mwe, and a $\cos^4$ variation at 598 mwe. Bollinger (1952) has measured the angular distribution of particles at 1600 mwe, with a hodoscoped counter telescope. His value for the cosine power is 3·1. As already stated, the total number of particles recorded by us is not quite sufficient to draw unambiguous conclusions regarding the exact power law obeyed by the underground particles.

(*C*) *Secondary production by μ-mesons*

At 22 mwe, about 5% of the mesons traversing the telescope produced secondaries such as knock-on's, bremsstrahlung electrons, etc., in the lead of our apparatus. The value increased to 18% at 1008 mwe (Table IV). These percentages are lower estimates, since the contribution from secondaries that pass through the same counters as the primaries could not be obtained. Tiffany and Hazen (1950) working with a cloud chamber at 860 mwe, have found a similar increase of secondary production. They found that at 860 mwe about 22% of μ-mesons traversing the chamber produced secondaries in the lead plates inside the chamber. Nassar and Hazen (1946) have found that the corresponding value at sea level is 6%. We can also compare the variation with depth, of the number of μ-mesons that are accompanied by secondaries, obtained in Section IV (B) (Table IV), with the theoretical prediction of Hayakawa and Tomonaga (1949). These authors have calculated the ratio of the number of electrons arriving at various depths accompanied by the generating mesons, to the total number of mesons at those depths. As explained in Section IV (B), our experiments give the percentage of mesons that arrive at various depths, accompanied by at least one secondary electron. The theoretical curve and the experimental points are plotted in Fig. 8. It is seen from the figure that the experimental values agree well with the theoretical values provided that mesons are accompanied mostly by single secondary electrons.

(*D*) *Energy spectrum of π-mesons and of μ-mesons*

In deducing the value of the exponent γ in the differential production spectrum of π-mesons, two assumptions were made:—(i) μ-Mesons are

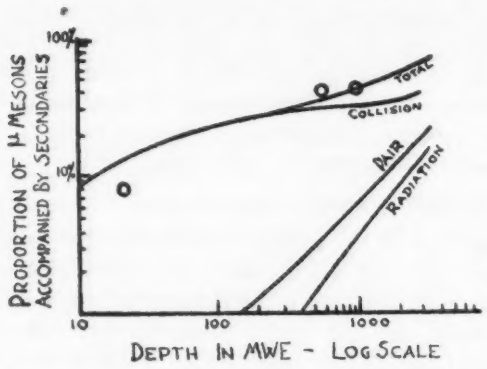

FIG. 8. Contribution of various processes (Collision, Pair production, and Radiation) to the equilibrium soft component at various depths.

produced only as a result of the decay of π-mesons; (ii) the cross-section for the absorption of π-mesons is nuclear geometric. It was reported at the Bristol Conference (December, 1951) by Perkins that at Bristol they had obtained evidence for the production of k-mesons along with the π-mesons, in high energy nuclear interactions, in the ratio $N_k/N_\pi = 0{\cdot}6 \pm 0{\cdot}2$. The average value of the mass of k-mesons given by them is $m_k = 1270\ m_e$. In a few cases they have identified the charged decay product of k-meson to be a μ-meson. If this result is established by further experiments, then our first assumption that μ-mesons result only as decay products of π-mesons is no longer tenable. It was shown in Section V that if we make the assumption that the μ-mesons observed underground are the decay products of π-mesons alone, then a π-meson production spectrum $dN_\pi\ (E) = k \cdot E^{-2{\cdot}4}$ reproduces the intensity-depth curve obtained by us. However, calculation shows that if we make the assumption that 50% of the mesons produced in nuclear interactions are k-mesons with a life-time $\leqslant 10^{-9}$ secs., then a much steeper production spectrum $dN_{\pi k}\ (E) = \text{constant} \cdot E^{-3{\cdot}0}$, will reproduce the observed intensity-depth curve.

Regarding the second assumption, it may be pointed out that the recent work of Lock and Yekutieli (1952) shows that the cross-section is nuclear geometric upto 1 Bev. Recent work in this Institute on production of stars in photographic emulsions by secondaries of penetrating showers, has revealed that the cross-section is of the same order (nuclear geometric) upto about 10^{12} ev. It seems therefore quite justifiable to assume the cross-section to be nuclear geometric for all energies considered by us.

Summary

An investigation on cosmic-ray intensity was carried out in the Gold Mines at Kolar (Mysore State), with a hodoscoped counter telescope, upto a depth of 1008 mwe. The following conclusions may be drawn from the investigation:—

(1) The intensity-depth curves for particles penetrating 2·5 cm. lead, and for those penetrating 10 cm. lead, run parallel between 500 and 1008 mwe.

(2) The vertical intensity of penetrating particles in terms of particles cm.$^{-2}$ sec.$^{-1}$ sterad^{-1} can be expressed by the power law $I_v = 10^{3.56} H^{-3.1 \pm 0.1}$ for $500 \leq H \leq 1008$ mwe.

(3) The flux values for the penetrating component obtained by us are higher than the flux values of the total component given by Wilson, by a factor 2, at all depths between 500 and 810 mwe. Our flux values for the penetrating component are higher than the corresponding flux values of Clay and Gemert by a factor 4·5. Our surface value of flux is in agreement with the surface values of Wilson, Clay and Gemert.

(4) The angular distribution follows approximately $\cos^3$ law at 22 mwe, and $\cos^4$ law at 598 mwe.

(5) The secondary production by μ-mesons in the lead of the apparatus, as well as the soft component that is in equilibrium with the hard component increases with depth. The experimental values giving the proportion of soft component that is in equilibrium with the penetrating component, agree well with the theoretical calculations of Hayakawa and Tomonaga.

(6) Assuming that all the μ-mesons observed underground are produced only as a result of the decay of π-mesons, the value of exponent in the differential spectrum of π-mesons at production in the energy range $200 < E < 450$ Bev, is found to be 2·4.

(7) The experimentally determined μ-meson integral spectrum in the energy range $150 < E < 300$ Bev is given by $N_\mu (> E) = 0{\cdot}664\, E^{-2.09 \pm 0.02}$.

(8) The neutral radiation underground is essentially of radioactive origin.

Acknowledgments

We wish to express our gratitude to Dr. H. J. Bhabha, for suggesting the investigation, and for helpful discussions. We are highly indebted to Dr. Bernard Peters for the valuable advice given in preparing this paper.

It is a pleasure to thank Dr. R. Ramanna for the help given to us in starting this work at Kolar.

We wish to express our grateful thanks to Messrs. John Taylor and Sons, for according permission to carry out the experiments in the Mines at the Kolar Gold Fields. We are especially grateful to Mr. V. M. Sundararajan, and Mr. T. C. Barnett of Nundydroog Mines for taking a lively interest in the investigation and for providing us with all the necessary facilities underground.

APPENDIX

The hodoscope photographs enable us to obtain a rough indication concerning the angular distribution of the particles passing through the telescope. For this purpose, we consider events of arrangement II, in which one counter in tray D, and one in tray B were discharged. The six D counters are denoted by symbols D_1, D_2, $\cdots D_6$ and the six B counters by symbols B_1, B_2, $\cdots B_6$. The event in which the i-th counter of tray D, and the j-th counter of tray B are discharged is denoted by (D_iB_j).

(D_1B_1), (D_2B_2), $\cdots (D_6B_6)$, *i.e.*, events belonging to the group $i-j=0$, are caused by particles arriving within an angle of 16° on either side of the vertical direction, in the plane perpendicular to the counter axes. Similarly, events of the group $i-j=\pm 1$, are due to particles arriving within an angular interval $\theta_{min.}=0°$, and $\theta_{max.}=31°$ on either side of the vertical, the mean direction in the interval, θ_m being $15\frac{1}{2}°$. Similarly for $i-j=\pm 2$ $\theta_{min.}=15\frac{1}{2}°$, $\theta_{max.}=42\frac{1}{2}°$, and $\theta_m=29°$, and for $i-j=\pm 3$, $\theta_{min.}=29°$, $\theta_{max.}=51°$, and $\theta_m=40°$.

In certain cases, the angle defined by a single counter in D and a single counter in B, is only insufficiently covered by the tray C. Therefore not all the events $i-j=0, \pm 1, \pm 2, \pm 3$, are necessarily recorded as ABCD coincidences. Table VI gives the combinations (D_iB_j) in the four groups $i-j=0, \pm 1, \pm 2, \pm 3$, which are fully covered by tray C. The number of particles counted in these four angular intervals at 22 and 598 mwe are given in columns 5, 6 of Table VI.

For comparison, these numbers have to be normalised using the factors 5·5, 8, 6 and 2, which are equal to the numbers of possible combinations (D_iB_j) for the four groups $i-j=0, \pm 1, \pm 2, \pm 3$. There is yet another normalisation factor arising out of the fact that the centres of the counters in B are not equidistant from the centre of any particular counter in D and *vice versa*. These factors are the geometric factors for the conversion

TABLE VI

Angular distribution of particles at 22 and 598 mwe

Mean Angle θ_m	Group	Types of events in the group (D_iB_j)	No. of combinations (D_iB_j)	No. of events observed at 22 mwe	No. of events observed at 598 mwe	No. of events normalised at 22 mwe	No. of events normalised at 598 mwe
0°	$i-j=0$	(D_1B_1), (D_2B_2), (D_3B_3) (D_4B_4), (D_5B_5), (D_6B_6)	5·5*	132	59	183 ±17	82 ±10
15½°	$i-j=\pm1$	(D_6B_5), (D_5B_4), (D_4B_3), (D_3B_2) (D_1B_2), (D_2B_3), (D_3B_4), (D_4B_5)	8·0	164	65	164 ±13	65 ±8
29°	$i-j=\pm2$	(D_6B_4), (D_5B_3), (D_4B_2) (D_3B_5), (D_2B_4), (D_1B_3)	6	90	28	135 ±14	42 ±8
40°	$i-j=\pm3$	(D_6B_3), (D_1B_4),	2	12	7	63 ±18	37 ±14

* Only three-fourths of the angles defined by (D_1B_1) and (D_6B_6) are covered by tray C.

of the observed intensities in various angular intervals into absolute intensities (in particles cm.$^{-2}$ sec.$^{-1}$ sterad^{-1}) in the mean directions joining the centres of the counters. The normalised figures giving the relative numbers of particles in the four directions $\theta_m = 0°$, $15\frac{1}{2}°$, 29°, and 40°, for depths 22 mwe, and 598 mwe are given in columns 7, 8 of Table VI, and plotted in Figs. 4, 5.

REFERENCES

Bollinger, L. M. .. (See George, E. P., 1952).

Clay, J. and Gemert, A. .. *Physica*, 1939 *b*, **6**, 497.

Daniel, R. R., Davies, J. H., Mulvey, J. H. and Perkins, D. H. *Bristol Conference on V-Particles and Heavy Mesons* December, 1951).

George, E. P. .. *Progress in Cosmic Ray Physics*, Ch. VII, p. 395, Ed. by J. G. Wilson (North Holland Pub. Co., 1952).

Greisen, K. I. .. *Phys. Rev.*, 1948, **73**, 521.

Hayakawa, S. and Tomonaga, S. *Prog. Theor. Phys.*, 1949, **4**, 496.

Lock, W. O. and Yekutieli, G. .. *Phil. Mag.*, 1952, **43**, 231.

Miesowicz, *et al.* .. *Phys. Rev.*, 1950, **77**, 380.

Miyazaki, Y. .. *Ibid.*, 1949, **76**, 1733.

Nassar, S. and Hazen, W. E. .. *Ibid.*, 1946, **69**, 298.

Tiffany, O. L. and Hazen, W. E. .. *Ibid.*, 1950, **74**, 849.

Wilson, Y. C. .. *Ibid.*, 1938, **53**, 337.

SOME REMARKS ON THE OPTICAL ROTARY DISPERSION OF QUARTZ

By S. Chandrasekhar

(From the Raman Research Institute, Bangalore)

Received June 20, 1952

(Communicated by Sir C. V. Raman, F.R.S., N.L.)

1. The Summation Rule in Rotary Dispersion

A fundamental theorem concerning the optical rotatory power of molecular systems was derived by Kuhn (1929), in the first instance, by considering the behaviour of a model consisting of two anisotropic linear resonators coupled with each other. The system is evidently capable of two modes of vibration both of which contribute to its rotatory power. But since the latter is a consequence of the interaction between the two resonators, the activity due to them turns out to be of opposite signs, when the frequency of the incident light is less than that of either resonator. For his elementary model, Kuhn derived the formula:

$$\rho = \left[\frac{1}{\nu_1^2 - \nu^2} - \frac{1}{\nu_2^2 - \nu^2}\right] a\nu^2, \tag{1}$$

where ρ is the optical rotatory power while ν_1 and ν_2 are the two characteristic frequencies of the model. Kuhn also showed that, more generally, we have

$$\rho = \sum_r \frac{a_r \nu^2}{(\nu_r^2 - \nu^2)},$$

where

$$\sum_r a_r = 0. \tag{2}$$

A proof of the summation rule (2) involving no special assumptions regarding the molecular model has been given by E. U Condon in his review article (1937). Discussing the quantum-mechanical theory of rotary dispersion due to Rosenfeld (1928), Condon has given the formula for the rotatory power

$$\rho = \frac{16\pi^3 N_1}{\lambda^2} \frac{n^2 + 2}{3} \beta, \tag{3}$$

where

$$\beta_a = \frac{c}{3\pi h} \sum_b \frac{R_{ba}}{\nu_{ba}^2 - \nu^2}, \tag{4}$$

β_a being the value of β appropriate to the molecules in quantum state a, R_{ba} being the rotational strengths of the line ν_{ba}. Condon has proved that the sum of the rotational strengths $\sum_b R_{ba}$ is equal to zero, which is true for all states, a, the summation being performed over all other states, b. This, in fact, is the same rule as that arrived at by Kuhn from his simple model.

It is clear, therefore, that the fundamental criterion about optical rotatory power furnished by the summation rule should be taken into account in deriving any formula, theoretical or empirical, which claims to express rotary dispersion. We shall proceed to examine the dispersion formulæ which had been proposed earlier, for quartz, in the light of these remarks.

2. The Earlier Rotary Dispersion Formulæ

Numerous formulæ have been proposed to account for the rapid increase in the rotatory power of quartz with decrease of wavelength. These formulæ include several terms both positive and negative, of the Drude type which are of the form

$$\rho = \sum_r \frac{Q_r}{\lambda^2 - \lambda_r^2} = \sum_r \frac{a_r \nu^2}{\nu_r^2 - \nu^2}, \tag{5}$$

where

$$Q_r = a_r \lambda_r^2 \tag{6}$$

These formulæ have been reproduced below. Throughout ρ is expressed in degrees per millimetre and λ in microns.

Drude's formula:

$$\rho = \frac{12{\cdot}2}{\lambda^2 - 0{\cdot}010627} - \frac{5{\cdot}046}{\lambda^2} \tag{7}$$

Lowry's first formula:

$$\rho = \frac{11{\cdot}6064}{\lambda^2 - 0{\cdot}010627} - \frac{4{\cdot}3685}{\lambda^2} + \frac{13{\cdot}42}{\lambda^2 - 78{\cdot}22} \tag{8}$$

Lowry's second formula:

$$\rho = \frac{9{\cdot}5639}{\lambda^2 - 0{\cdot}0127493} - \frac{2{\cdot}3113}{\lambda^2 - 0{\cdot}000974} - 0{\cdot}1905 \tag{9}$$

Bradshaw and Livens's formula:

$$\rho = \frac{845{\cdot}694}{(\lambda^2 - 0{\cdot}01274912)} - \frac{0{\cdot}40235}{(\lambda^2 - 0{\cdot}01274912)^2} - \frac{838{\cdot}432}{(\lambda^2 - 0{\cdot}0120800)} - \frac{0{\cdot}1331233}{(\lambda - 0{\cdot}0120800)^2} + \frac{43{\cdot}05794}{(\lambda^2 - 80{\cdot}00)} + \frac{2119{\cdot}117}{(\lambda^2 - 80{\cdot}00)^2} \tag{10}$$

Radhakrishnan's formula:

$$\rho = \frac{4\cdot948}{(\lambda^2 - 0\cdot014161)} + \frac{4\cdot617}{\lambda^2 - 0\cdot011236} - \frac{2\cdot311}{\lambda^2 - 0\cdot000974} - \frac{0\cdot000815}{(\lambda^2 - 0\cdot0195)^2} - 0\cdot1905 \qquad (11)$$

As mentioned in an earlier paper (Chandrasekhar, 1952), all these formulæ, except Radhakrishnan's, deviate from the experimental data as we proceed into the ultraviolet. We shall now test whether these formulæ satisfy the summation rule which we have referred to in the previous section. Taking into consideration only the absorption bands in the visible and ultraviolet, $\Sigma_r a_r$ has been evaluated for all these formulæ making use of the relation $a_r = Q_r/\lambda_r^2$. In formulæ (7) and (8), the summation condition clearly does not hold, for, a_r becomes very large for the terms for which λ_r is considered as vanishingly small. In formulæ (9) and (11) also, $\Sigma_r a_r$ for the terms of the Drude type does not vanish, the negative strength being nearly three times as great as the positive strength in both cases. In Bradshaw and Livens's formula (10), the rotatory power is expressed principally as a difference of two very large terms of the Drude type, involving two close absorption wavelengths. Here again the summation condition is found to fail since $\Sigma_r a_r$ for the Drude terms is negative and of the same order of magnitude as for formulæ (9) and (11). *Thus we find that the formulæ* (7) *to* (11) *which have been proposed do not satisfy the basic requirement of the theory and hence are inappropriate.*

3. THE AUTHOR'S FORMULA

The present author has shown (Chandrasekhar, *loc. cit*) that the rotary dispersion of quartz is well represented throughout the visible and ultraviolet range of the spectrum by the single-term formula

$$\rho = \frac{K\lambda^2}{(\lambda^2 - \lambda_0^2)^2}, \qquad (12)$$

where

$$K = 7\cdot186 \text{ and } \lambda_0 = 0\cdot0926283\,\mu.$$

It will be shown that the above formula satisfies the summation rule which, as shown above, disqualifies the earlier formulæ for quartz. For, let us consider the limiting case in Kuhn's formula (1), when ν_1 and ν_2 are nearly equal. Then, the formula reduces to

$$\rho = \frac{a\epsilon\nu^2}{(\nu_0^2 - \nu^2)^2} = \frac{K\lambda^2}{(\lambda^2 - \lambda_0^2)^2}$$

neglecting $\epsilon^2/4$ in the denominator,

where

$$\epsilon = \nu_2^2 - \nu_1^2$$

and

$$\nu_0^2 = \frac{\nu_1^2 + \nu_2^2}{2} .$$

Such a case, when ν_1 is nearly equal to ν_2, would arise when the two resonators in Kuhn's model are identical, so that when they are feebly coupled there would be two modes of vibration for the system whose frequencies would form a close doublet. This, in fact, supports the statement made by the author in his previous paper (*loc. cit.*) that the accuracy of fit of the above formula for quartz indicates that its optical activity arises as a result of an interaction in the nature of resonance between similar units constituting the crystal.

4. Rotary Dispersion Normal to the Optic Axis

The rotary dispersion of quartz at right angles to the optic axis has been determined for several wavelengths from 5461 A.U. to 2537 A.U. by Bruhat and Grivet (1935). It is found that the rotatory power in this direction ($\rho_\perp$) is opposite in sense to the rotatory power along the optic axis ($\rho_\parallel$) and that $\rho_\perp/\rho_\parallel$ is approximately constant over this range of wavelengths. The data are well represented by a formula of the same general form (12) when $K = -3{\cdot}56$ and $\lambda_0 = 0{\cdot}111355\,\mu$. The calculated and experimental values are given in Table I below.

Table I

Rotary Dispersion normal to the Optic Axis

λ (in μ)	ρ (expt.)	ρ (calc.)
·2537	−86	−84·9
·2653	−74·5	−74·5
·2804	−63	−63·8
·3021	−51	−52·2
·3128	−48	−47·7
·3341	−40·5	−40·4
·3665	−32	−32·3
·4047	−26	−25·4
·4358	−21·5	−21·5
·5461	−13	−13·0

It will be seen from the above table that the calculated values agree with the experimental data over the whole range of wavelengths within the limits of experimental error. A comparison with the formula along the optic axis shows that the constant in the numerator in the present case is reduced by about $\frac{1}{2}$, but the characteristic absorption wavelength λ_0 is slightly increased. This is not surprising, for even in the case of ordinary refraction, it is well known that the dispersion formulæ are notably different for different directions in the crystal.

In conclusion, I wish to record here my sincere thanks to Prof. Sir C. V. Raman, KT., N.L., F.R.S., for the helpful hints he gave me during this investigation.

5. SUMMARY

The quantum mechanical theory of rotary dispersion leads to the rule that the sum of the rotational strengths $\Sigma_r a_r$ of the various terms in a dispersion formula of the Drude type expressed in terms of the characteristic frequencies should be zero. It is shown in this paper that the rotary dispersion formulæ for quartz which had been proposed earlier do not satisfy this summation rule. On the other hand, the single-term formula of the form $\rho = K\lambda^2/(\lambda^2 - \lambda_0^2)^2$ suggested by the present author which fits the data along the optic axis accurately from the visible to the ultra-violet region of the spectrum, fulfils the summation condition. It is also shown that the data of Bruhat and Grivet for the rotary dispersion of quartz normal to the optic axis is fitted well by a formula of the same form as that given above if we put $K = -3{\cdot}56$ and $\lambda_0 = 0{\cdot}111355\,\mu$.

REFERENCES

1. Bruhat, G. and Grivet, P. .. *J. de Phy.*, 1935 (7), **6**, 12.
2. Chandrasekhar .. *Proc. Ind. Acad. Sci.*, 1952, **35 A**, 103.
3. Condon, E. U. .. *Rev. Mod. Phys.*, 1937, **9**, 432.
4. Kuhn, W. .. *Z. f. Physik. Chemie*, 1929, **4 B**, 14.
5. Rosenfeld, L. .. *Z. f. Phys.*, 1928, **52**, 161.

VOLUMETRIC DETERMINATION OF MANGANESE WITH 8-HYDROXY-QUINOLINE

By K. Neelakantam, F.A.Sc. and K. Parthasarathi
(*Department of Chemistry, Andhra University, Waltair*)

Received April 18, 1952

Berg[1] carried out the precipitation of manganese oxinate in two ways. In the first method, precipitation was carried out from an acetic acid-sodium acetate buffered solution containing a reducing agent by adding an alcoholic solution of oxine and in the second, the mineral acid solution containing manganese and oxine, without any reducing agent, was treated with dilute ammonia. The conditions for the precipitation of the complex were studied by Taylor-Austin,[2] Goto,[3] Tsinberg,[4] Smith[5] and Neelakantam.[6] The last author showed that the precipitates obtained by the second method could be dried to constant weight at 150° C., contrary to the statement of Berg, and recommended this method of precipitation.

The volumetric estimation was carried out both by the direct and indirect methods by Berg.[1] In the direct method the complex precipitated by one of the above methods was dissolved in hydrochloric acid and titrated bromatometrically in the usual manner. In the indirect method, the complex was precipitated by adding an excess (measured volume) of the reagent and the excess determined in the filtrate. Excellent results were recorded in both cases.

Neelakantam[6] reported that appreciable adsorption of oxine by the precipitate occurred when the precipitation was carried out in the presence of an excess of the reagent, with or without the addition of strong ammonia, and that a double precipitation did not improve the accuracy of the results in such cases. In the present investigation, the volumetric estimation of manganese under the conditions which occur in rock analysis was studied with special reference to the direct and indirect methods of titration suggested by Berg and their accuracies evaluated by comparison with the gravimetric method of Neelakantam.[6]

Experimental

Manganous Chloride.—Crystalline manganous chloride ($MnCl_2$, 4 H_2O; A.R.) was dissolved in water and acidified with hydrochloric acid to prevent hydrolysis. The stock solution was standardised by the oxine method

(gravimetric) proposed by Neelakantam[6] and the results checked up against the pyrophosphate method.

Oxine Solution.—A solution of oxine (2·5%) in acetic acid (2 N) was prepared.

Standard Bromate-Bromide (0·1 N).—Potassium Bromate (A.R. quality, 2·784 gm.) was accurately weighed out, dissolved in water along with potassium bromide (12 gm.) and made upto one litre.

Standard Sodium Thiosulphate (0·1 N).—Crystalline sodium thiosulphate (A.R. quality; 25 gm.) was dissolved in water and made up to one litre. The solution was standardised against the standard bromate solution in the usual manner.

Procedure: *Direct Method.*—The oxinate complex was precipitated according to the procedure recommended by Neelakantam.[6] In the volumetric method the precipitate was dissolved in hot dilute hydrochloric acid (2 N) and the liberated oxine determined bromatometrically in the following manner:—

The cold solution was treated with 3 drops of indigo carmine solution (1%) and titrated with standard bromate-bromide mixture slowly until the solution became pure yellow. The solution was diluted with 50 c.c. of dilute acid (2 N) and treated with 10 c.c. of potassium iodide solution (10%). The liberated iodine was titrated with standard thiosulphate, starch being added towards the end of titration.

The effect on the accuracy of the volumetric results of the following factors was investigated:—(*a*) magnitude of the excess oxine, (*b*) strong ammonia added after precipitation, and (*c*) presence of sodium chloride in large proportion.

Effect of Excess Oxine.—A measured volume of the oxine solution (2·5%) was added in excess of the theoretical requirement and precipitation carried out with dilute ammonia. Duplicate gravimetric and volumetric estimations were carried out. The results are given in Table I.

The results in Table I show clearly that both in the gravimetric and volumetric methods the errors are positive and tend to gradually increase with the excess oxine added. However, the volumetric method yields slightly higher values.

Effect of Strong Ammonia.—Precipitation was carried out using a slight excess (1 c.c.) of the reagent and dilute ammonia. Finally a measured volume of liquor ammonia was added. The determination was completed volumetrically. The results are given in Table II.

TABLE I

Manganese taken = 0·0575 gm.

No.	Oxine excess (c.c.)	Manganese Found (gm.)	
		Gravimetric	Volumetric
1	1·0	0·0575	0·0577
2	2·0	0·0578	0·0578
3	4·0	0·0578	0·0580
4	6·0	0·0579	0·0582

TABLE II

Manganese taken = 0·0575 gm.

No.	Liquor Ammonia (c.c.)	Manganese Found (gm.)	Error (mg.)
1	5·0	0·0580	+0·5
2	10·0	0·0581	-0·6
3	15·0	0·0583	+0·8
4	20·0	0·0585	+1·0

The above results show clearly that adsorption rapidly increases with the amount of liquor ammonia added.

Effect of Excess Oxine and Strong Ammonia.—Precipitation was carried out in presence of a measured excess of the oxine reagent by adding dilute ammonia and 20 c.c. of liquor ammonia was gradually added in each case. The determination was completed volumetrically. The results are given in Table III.

The adsorption of oxine is very strong. With excess of the reagent, the complex was obtained as a pasty mass which turned into a hard mass on boiling. Satisfactory washing of the precipitate was impossible.

TABLE III

Manganese taken = 0·0575 gm.

No.	Oxine excess (c.c.)	Manganese Found (gm.)	Error (mg.)
1	7·0	0·0585	+1·0
2	10·0	0·0593	+1·8
3	13·0	0·0594	+1·9
4	16·0	0·0625	+5·0

Effect of Sodium Chloride.—Precipitation was carried out in presence of 15 gm. of sodium chloride with a measured excess of oxine and dilute ammonia. The determination was completed volumetrically. The results are given in Table IV.

TABLE IV

Manganese taken = 0·0575 gm.

No.	Oxine excess (c.c.)	Manganese Found (gm.)	Error (mg.)
1	2·0	0·0574	−0·1
2	6·0	0·0575	Nil
3	10·0	0·0575	Nil
4	14·0	0·0582	+0·7

The above results compared with those given in Table I show clearly that the magnitude of the adsorption is lesser in presence of sodium chloride for the same excess oxine added.

From the above data it is clear that the direct titration method yields satisfactory results provided a large excess either of oxine or ammonia is not used in the precipitation.

Back Titration Method.—The manganese was precipitated under the conditions referred to above using a measured volume (excess) of a standard oxine solution from a burette. The precipitate was filtered through a

Whatman No. 41 paper and washed with hot water. The cold filtrate was made upto 500 c.c. in a measuring flask and aliquot portions titrated for excess oxine with bromate-bromide in the usual manner. The manganese content was calculated from the oxine used up. The results are given in Table V.

TABLE V

Manganese taken = 0·0575 gm.

No.	Oxine (c.c.)	Manganese Found (gm.)	Error (mg.)
1	19·0	0·0621	+ 4·6
2	23·0	0·0617	+ 4·2
3	27·0	0·0626	+ 5·1
4	31·0	0·0684	+10·9

The excess (over the theoretical requirement) of oxine used ranges from 6·5 to 18·5 c.c. in the above experiments. The errors are large, and this shows that the excess of oxine was not completely removed inspite of repeated washing. It was also noticed in the latter experiments that the precipitate was obtained as a pasty mass which became solid on heating. The magnitude of the excess used is normal to a back titration method. The back titration method is therefore unsatisfactory.

SUMMARY

The volumetric determination of manganese with 8-hydroxy-quinoline was investigated. Errors due to adsorption have been shown to increase with increase in (*a*) amount of excess reagent and (*b*) strong ammonia; and to decrease in presence of sodium chloride. The direct titration method was found to yield satisfactory results provided a large excess of oxine or ammonia was not used. The back titration method was found to yield very high values due to adsorption.

REFERENCES

1. Berg .. *Zeit. anal. Chem.*, 1929, **76**, 191.
2. Taylor-Austin .. *Analyst*, 1938, **63**, 571, 710.
3. Goto .. *Chem. Abs.*, 1938, **32**, 2863.
4. Tsinberg .. *Ibid.*, 1938, **32**, 449.
5. Smith .. *Analyst*, 1939, **64**, 787.
6. Neelakantam .. *Proc. Ind. Acad. Sci.*, 1948, **27 A**, 202.

ON RECURRENCE RELATIONS INVOLVING LEGENDRE'S ASSOCIATED FUNCTIONS OF ONE KIND ONLY

By Y. V. Thosar, M.Sc.

(*Department of Mathematics, College of Science, Nagpur*)

Received February 20, 1952

(Communicated by Prof. B. S. Madhava Rao)

§ 1. It is well known that Legendre's associated functions $P_n^m(z)$ satisfy the following four linear differential-difference relations:*

$$(1) \quad (n+m)\,P_{n-1}^m = nz\,P_n^m - (z^2-1)(P_n^m)',$$

$$(2) \quad (n-m+1)\,P_{n+1}^m = (n+1)\,z\,P_n^m + (z^2-1)(P_n^m)',$$

$$(3) \quad (n-m+1)(n+m)\,P_n^{m-1} = (z^2-1)^{\frac{1}{2}}(P_n^m)' + mz(z^2-1)^{-\frac{1}{2}}P_n^m,$$

$$(4) \quad P_n^{m+1} = (z^2-1)^{\frac{1}{2}}(P_n^m)' - mz(z^2-1)^{-\frac{1}{2}}P_n^m.$$

These and fourteen other recurrence relations involving the $P_n^m(z)$ have been listed by Ganesh Prasad.[1] Shabde[2] has studied independent proofs of nine of them, and by combining two or more of these nine relations (which include the above four) he has deduced the remaining nine. The object of the present note is to point out that the above four relations would entirely suffice to deduce all the others. It thus appears to be superfluous to study independent proofs of all the nine relations apparently considered by Shabde as basic. A few other relations have been deduced likewise which would well fit into the list drawn up by Ganesh Prasad.

§ 2. The nine relations taken as basic by Shabde are the relations (1)–(4) above and the following five:

$$(5) \quad (n-m+1)\,P_{n+1}^m - (2n+1)\,z\,P_n^m + (n+m)\,P_{n-1}^m = 0,$$

$$(6) \quad P_n^{m+1} + 2mz(z^2-1)^{-\frac{1}{2}}P_n^m - (n-m+1)(n+m)P_n^{m-1} = 0$$

$$(7) \quad (z^2-1)^{\frac{1}{2}}P_n^{m+1} - (n-m)\,z\,P_n^m + (n+m)\,P_{n-1}^m = 0,$$

$$(8) \quad (n+m)(z^2-1)^{\frac{1}{2}}P_n^{m-1} + z\,P_n^m - P_{n+1}^m = 0,$$

$$(9) \quad (n+1)\,P_{n+1}^m - m(n+m)(z^2-1)^{\frac{1}{2}}P_n^{m-1} - (z^2-1)^{\frac{1}{2}}P_n^{m+1} = (n+2m+1)\,z\,P_n^m.$$

---

* Throughout this note, n, m and z are arbitrary complex; the unwritten argument z is to be understood and dashes denote differentiation with respect to z.

The relations (5)–(9) are all trivially derivable from the relations (1)-(4): thus the elimination of $(P_n^m)'$ from (1) and (2), from (3) and (4), from (1) and (4), from (2) and (3) would respectively yield the relations (5), (6), (7), (8); and finally the substitution in the left member of (9) from (2), (3), (4) respectively for P_{n+1}^m, P_n^{m-1}, P_n^{m+1} would establish (9).

One can similarly verify the following new relations by substitution from (1), (2), (3), (4), respectively for P_{n-1}^m, P_{n+1}^m, P_n^{m-1}, P_n^{m+1}:

(10) $(z^2-1)^{\frac{1}{2}} P_n^{m+1} + (n+m+1)\, z\, P_n^m - (n-m+1)\, P_{n+1}^m = 0,$

(11) $(2n+1)(z^2-1)(P_n^m)' = n(n-m+1) P_{n+1}^m - (n+1)(n+m) P_{n-1}^m,$

(12) $(z^2-1)(P_n^m)' = n(n-m+1)(z^2-1)^{\frac{1}{2}} P_n^{m-1} - m P_{n-1}^m,$

(13) $(n-m)(z^2-1)(P_n^m)' = n(z^2-1)^{\frac{1}{2}} P_n^{m+1} + m(n+m) P_{n-1}^m,$

(14) $(z^2-1)(P_n^m)' = (n+1)(n+m)(z^2-1)^{\frac{1}{2}} P_n^{m-1} - m P_{n+1}^m,$

(15) $(n+m+1)(z^2-1)(P_n^m)' = m(n-m+1) P_{n+1}^m + (n+1)(z^2-1)^{\frac{1}{2}} P_n^{m+1},$

(16) $2m(z^2-1)^{-\frac{1}{2}} P_{n+1}^m = (n+m)(n+m+1) P_n^{m-1} - P_n^{m+1},$

(17) $2m(z^2-1)^{-\frac{1}{2}} P_{n-1}^m = (n-m)(n-m+1) P_n^{m-1} - P_n^{m+1},$

(18) $(2n+1)(z^2-1)^{\frac{1}{2}} P_n^{m+1} = (n-m)(n-m+1) P_{n+1}^m - (n+m)(n+m+1) P_{n-1}^m.$

The above relations (10)–(18) are analogous to some of the relations recorded by Ganesh Prasad and might be considered to be a contribution to his list. It would be easy to extend the list of such relations to any length by only making use of the standard relations (1)–(4) in various combinations.

It may be added in conclusion that all the relations considered in this note hold also if the $P_n^m(z)$ are replaced by the corresponding $Q_n^m(z)$, since the standard relations (1)–(4) are the same for the Q's as for the P's.

References

1. Ganesh Prasad .. *A Treatise on Spherical Harmonics*, Part II, 1932, 83–86.
2. Shabde, N. G. .. *Proc. Ben. Math. Soc.*, 1931, **12.**

A NOTE ON THE BIOGENESIS OF PEDICIN

By G. Venkat Rao and T. R. Seshadri, F.A.Sc.

(From the Department of Chemistry, Delhi University)

Received April 9, 1952

In an earlier publication[1] the biogenesis of pedicin was considered to involve the following steps.

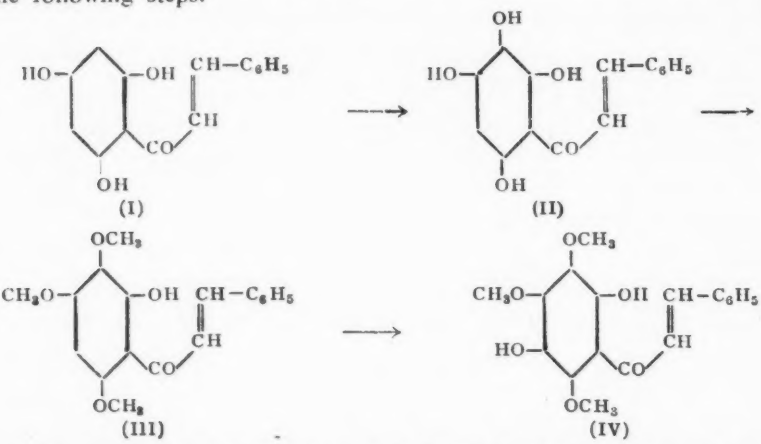

The possibility of oxidation of (I) to (II) can be granted based on well-known analogies, the conversion of (III) to (IV) was effected by nuclear oxidation using alkaline persulphate.[1] An important point that required to be established was the conversion of (II) to (III) by partial methylation. That this is the course of the reaction and not the alternative, *i.e.*, formation of 2-hydroxy-4 : 5 : 6-trimethoxy chalkone was not proved. In order to provide this proof the study of the partial methylation of a closely related but simpler case has now been undertaken. When 2 : 3 : 6-trihydroxy-4-methoxy acetophenone (VII), prepared from 2-hydroxy-3 : 4 : 6-trimethoxy acetophenone (V) by first carrying out oxidative demethylation to the quinone[2] (VI) and subsequent reduction with sodium hydrosulphite, is methylated with two moles of dimethyl sulphate the original 2-hydroxy-3 :4 : 6-trimethoxy acetophenone (V) is obtained. Hence the validity of the biogenetic scheme is supported. It has not been possible to prove the above point strictly using the corresponding chalkone (X) itself since it is unstable and undergoes change into the corresponding flavanone. But the manner of flavanone ring closure again supports the greater reactivity of the hydroxyl in the 6-position, since the product is found to be 7-methoxy-5 : 6-dihydroxy flavanone (XI).

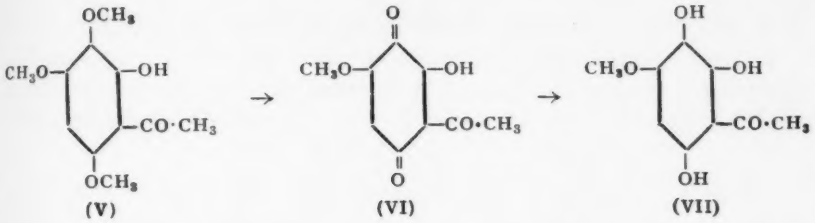

(V) (VI) (VII)

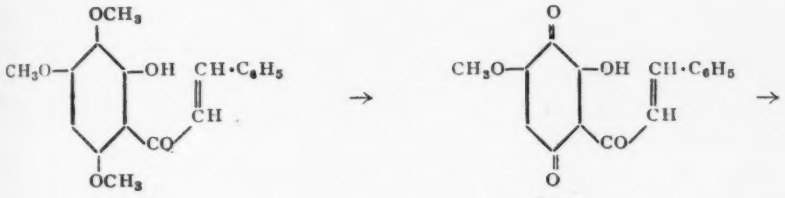

(VIII) (IX)

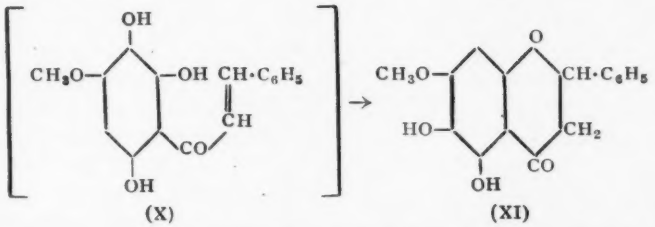

(X) (XI)

On account of the instability of chalkones having hydroxyl groups in the 2- and 6-positions and of the greater stability of flavanones having a hydroxyl group in the 5-position, an alternative scheme of biogenesis would suggest itself as more probable and is given below. 5 : 7-Dihydroxy flavanone (XII) represents a type which is widely distributed. When it undergoes nuclear oxidation it can give rise to (XIII) which belongs to the carthamidin type. If all the hydroxyl groups of this compound should be methylated then the ring structure would become unstable and the corresponding chalkone (III) would be produced which on further nuclear oxidation would give rise to pedicin.

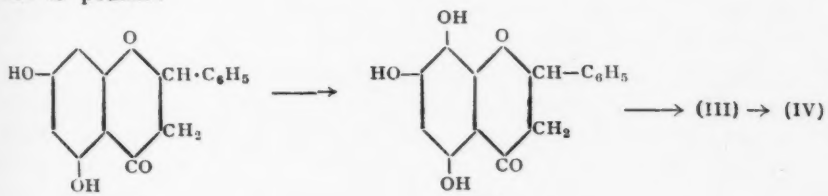

(XII) (XIII)

EXPERIMENTAL

2 : 3 : 6-*Trihydroxy*-4-*methoxy acetophenone* (*VII*).—This was first prepared by Rao, Rao and Seshadri.[2] Their procedure has now been followed except for the last stage *i.e.*, the reduction of the quinone (VI) to the final product.

2-Hydroxy-4-methoxy-3 : 6-quinoacetophenone (VI) (5 g.) was added to boiling water (60 c.c.) followed by sodium hydrosulphite (10 g.) in small quantities. A clear solution was obtained which was boiled for further two minutes and quickly cooled under the tap when a pale yellow solid separated. It was filtered, washed with cold water and crystallised from dry benzene when the quinol was obtained as pale yellow prismatic needles melting at 170–1°; yield, 3 g.

The triacetate of this compound was prepared using acetyl chloride and a drop of pyridine and heating under reflux on a water-bath for an hour. It crystallised from dry benzene as colourless prismatic tablets, melting at 184–5°. (Found: C, 55·8; H, 4·8; $C_{15}H_{16}O_8$ requires C, 55·6; H, 4·9%.)

Partial methylation of 2 : 3 : 6-*trihydroxy*-4-*methoxy acetophenone* (*VII*).—The above quinol (1 g.) was dissolved in dry acetone (50 c.c.) and redistilled dimethyl sulphate (1 c.c.; 2·1 moles) and ignited potassium carbonate (5 g.) were added. The mixture was refluxed for 12 hours, the acetone solution was filtered hot and the potassium salts washed with hot acetone. The solvent was distilled off from the filtrate and the residue dissolved in benzene and extracted with dilute sodium hydroxide (5%) twice. The alkaline extract was cooled in ice and ice-cold concentrated hydrochloric acid was then added in excess and left overnight in the ice-chest. The solid that separated out was filtered and crystallised from benzene when 2-hydroxy-3 : 4 : 6-trimethoxy acetophenone (V) was obtained, m.p. 113°; the mixed melting point with an authentic sample was undepressed.

Reduction of 2-*hydroxy*-4-*methoxy*-3 : 6-*quino-chalkone* (*IX*).—The chalkone (VIII) was prepared by the method of Rao and Seshadri,[1] and oxidised to the quino-chalkone (IX) by the method of Rao, Rao and Seshadri.[2] Its reduction did not proceed satisfactorily with sodium hydrosulphite. Stannous chloride[3] was found to be suitable.

2-Hydroxy-4-methoxy-3 : 6-quino-chalkone (IX) (1 g.) was dissolved in alcohol (100 c.c.) and the solution boiled under reflux. To this was added in small quantities a solution of pure stannous chloride (25 g.) in concentrated hydrochloric acid (20 c.c.) during the course of one hour while the mixture was kept refluxing. The heating was continued for another hour.

The initial dark brown colour of the mixture gradually became pale yellowish brown. The alcohol was then distilled off as much as possible under reduce-pressure and the brown solution left behind was diluted with water (100 c.c.). The brown yellow solid that separated out was filtered, washed with water and dried in a vacuum desiccator. The product crystallised from ethyl acetate as pale yellow large prisms melting at 248° (decom.) with sintering at 225°. It gave a bright green colour with alcoholic ferric chloride slowly changing to brown with excess of the reagent and no colour with alcoholic solution of *p*-benzoquinone. These reactions agreed with the requirements of a 5: 6-dihydroxy flavanone structure. The compound was found to be identical with 5: 6-dihydroxy-7-methoxy flavanone (IX) obtained by another method (unpublished results) and the mixed melting point was undepressed.

Summary

Of the two hydroxyl groups in the 2- and 6-positions of 2: 3: 6-trihydroxy-4-methoxy acetophenone and chalkone the 6-hydroxyl is shown to be more reactive. A modified biogenetic scheme is suggested for pedicin.

References

1. Rao and Seshadri .. *Proc. Ind. Acad. Sci.*, 1948, **27 A**, 375.
2. Rao, Rao and Seshadri .. *Ibid.*, 1948, **27 A**, 245.
3. Salooja, Sharma and Siddiqui *Journ. Sci. Indust. Res.*, 1947, **6 B**, 57.

SYNTHETIC EXPERIMENTS IN THE BENZOPYRONE SERIES

Part XVIII. Use of N-Bromo-Succinimide for the Synthesis of Flavones

By N. R. Bannerjee and T. R. Seshadri, F.A.Sc.

(From the Department of Chemistry, Delhi University, Delhi)

Received April 15, 1952

The conversion of flavanones into flavones has been considered in an earlier publication.[1] The use of bromine was one of the earliest methods examined. Methoxy-flavanones first used by Kostanecki[2] underwent nuclear bromination besides substitution in the 3-position. More recently, Zemplen[3] employed acetates for this purpose, bromination being carried out in the presence of ultra-violet light. By this means, he obtained 3-bromo-derivatives without nuclear bromination. The use of N-bromo-succinimide, instead of bromine, appeared to provide a good improvement and probably be free from complications. Bromination of cyclohexanone[4] in the α-position by means of this reagent is already known and the product is α-bromo-cyclohexanone which yields subsequently cyclohexenone on treatment with bases for the removal of hydrogen bromide. Tetra-hydro-γ-pyrone is similarly reported to give 50% yield of the 3 : 5-dibromo-derivative[5] which could be converted into γ-pyrone on treatment with pyridine. An analogous series of reactions would give rise to a flavone from a flavanone.

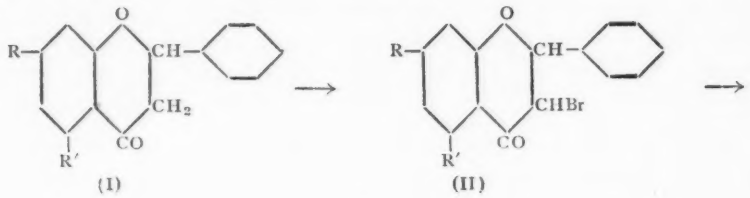

(*a*) R=OCH_3, R′=H (*b*) R=R′=OCH_3

As the simplest case, 7-methoxy-flavanone (I *a*) has now been first examined, the reaction with N-bromo-succinimide being activated by the addition of benzoyl peroxide. The resulting bromo-compound (II *a*) is directly treated with dilute alcoholic sodium hydroxide solution and the final product is found to be identical with 7-methoxy-flavone (III *a*). When 5: 7-dimethoxy-flavanone (I *b*) is used in stead, the product is a mixture involving some nuclear bromination also; the bromo-compounds can be separated into two fractions using ethyl acetate. The less soluble fraction crystallises in colourless needles melting at 206–7°. It is found to be a mono-bromo-flavanone (IV) and gives rise to the corresponding mono-bromo-chalkone (V) when treated with alcoholic sodium hydroxide solution, showing thereby, that only nuclear bromination has taken place. The more soluble fraction on treatment with alcoholic sodium hydroxide solution and careful crystallisation yields a mono-bromo-flavone (VII) in small quantities showing that in this case, besides nuclear bromination the 3-position has also been substituted (VI). The above nuclear bromination can probably be attributed to the influence of the activator benzoyl-peroxide, and was previously observed in the reaction with 3-methyl benzofuran.[6] In the present case, it seems to be more prominent than bromination of the methylene group since the mixture of products contains nuclear brominated (monobromo) flavanone (IV) along with another having substitution in the 3-position besides the nuclear bromination (VI). In regard to the position of the bromine atom in the benzene nucleus, it could be surmised that it is most probably in the 8-position. The relevant considerations would be as follows. With 7-methoxy

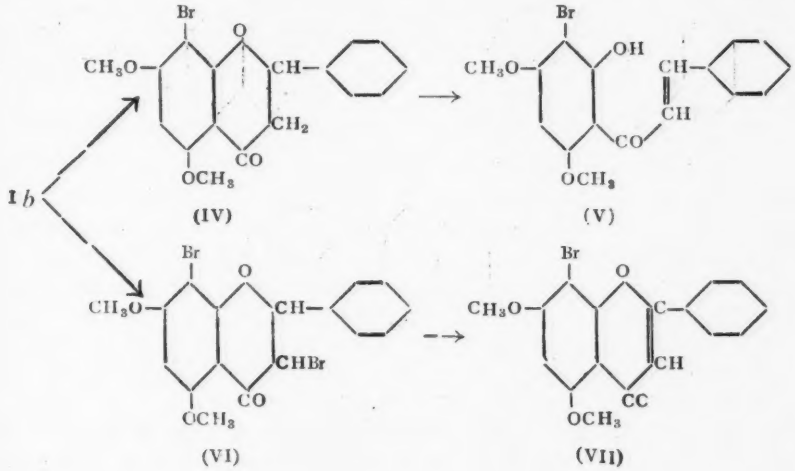

flavanone, no nuclear bromination takes place. Hence 7-methoxyl group is not taking an active part in nuclear substitution, probably because the position *para* to it is not available for this purpose. 5-Methoxyl group should therefore be responsible for this nuclear substitution and 8-position which is *para* to it is the most likely position to be concerned. Similar results have been obtained in the case of coumarins.

As representative of acetates which could be expected to resist nuclear bromination, naringenin acetate[7] (VIII) has next been examined. There has been considerable difficultly in preparing this acetate in a pure condition owing to the tendency of the pyranone ring to open and yield the corresponding chalkone acetate. It has now been most conveniently prepared by acetylation of naringenin using acetyl chloride and pyridine in the cold. When this acetate is boiled with N-bromo-succinimide in carbon tetrachloride solution in the presence of benzoyl peroxide it gives rise to a mixture of products. The more sparingly soluble fraction (major fraction) is free from bromine and is found to consist of apigenin triacetate (IX) which should arise from the bromination of the flavanone in the 3-position and the subsequent spontaneous elimination of hydrogen bromide under the conditions of bromination itself. This kind of spontaneous elimination of hydrogen bromide has been noted earlier in the case of bile acids.[8] The more soluble fraction (minor fraction) contains bromine and yields on treatment with alcoholic alkali apigenin; hence this fraction should consist of 3-bromo-naringenin triacetate (VIII *a*).

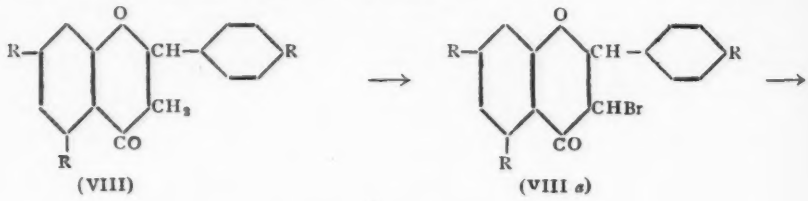

(VIII) (VIII *a*)

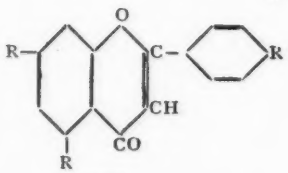

(IX)

R= —O·CO·CH$_3$

The results given above lead to the conclusion that the N-bromo-succinimide method is not invariably satisfactory with methyl ethers of flavanones

since without peroxides the reaction is very slow and in their presence nuclear bromination also takes place. On the other hand, the method seems to be quite suitable for the conversion of acetates of hydroxy flavanones to the corresponding flavone acetates.

Experimental

Action of N-Bromo-Succinimide on

(1) *7-Methoxy-flavanone* (*I a*)

7-Methoxy-flavanone (1·05 g.), N-bromo-succinimide (0·73 g.) and benzoyl peroxide (0·05 g.) were dissolved in anhydrous, distilled carbon tetrachloride (50 c.c.) and the mixture was refluxed on a steam-bath. The solution assumed a reddish-brown colour very soon and a flocculent precipitate having the same colour appeared within 10 minutes. Within half an hour the colour of the solution disappeared and the precipitate also became colourless and crystalline within about an hour. No hydrogen bromide appeared to be evolved. The mixture was then cooled in ice, the succinimide that had separated out was filtered and washed with a little solvent and the collected filtrate was then distilled to remove the solvent. The semi-solid mass was washed with hot water thrice to remove all succinimide and then it solidified. It was subsequently treated with cold alcoholic sodium hydroxide (20 c.c., 2%) for one hour and the solution diluted with water when the final product separated out as colourless needles. It was filtered, washed with water in order to free it from alkali and dried. It crystallised from ethyl acetate-petroleum ether mixture in long, colourless needles melting at 109–10°. Mixed melting point with an authentic sample of 7-methoxy-flavone (III *a*) was not depressed. Yield, 0·62 g.

(2) *5: 7-Dimethoxy-flavanone* (I *b*)

5: 7-Dimethoxy-flavanone (0·73 g.), N-bromo-succinimide (0·46 g.) and benzoyl peroxide (0·03 g.) were taken in anhydrous carbon tetrachloride (50 c.c.) and refluxed on a steam-bath for about 4 hours. The solution assumed a pale-yellow colour in about 1 hour and remained permanent light-yellow at the end of the reaction. The mixture was cooled in ice and the succinimide that separated out was filtered off and washed with a little carbon tetrachloride and then the solvent was distilled off from the filtrate. A pale-yellow solid was left behind. It was crystallised from ethyl acetate thrice when colourless needles melting at 206–7° were obtained. Yield, 0·12 g. (Found: C, 55·6; H, 4·2; $C_{17}H_{15}O_4Br$ requires C, 56·2; H, 4·1%). This was mono-bromo-flavanone (IV).

The above compound (75 mg.) was dissolved in alcohol (10 c.c.) and alcoholic sodium hydroxide solution (10 c.c., 4%) added and the mixture was allowed to stand in the cold for 2 hours and then diluted with water. Nothing separated out. The solution was then acidified with dilute hydrochloric acid when a yellow solid separated out. It was filtered, dried at room temperature and then crystallised from benzene when it came out as stout, rectangular prisms melting at 182–4°. It gave a brown colouration with alcoholic ferric chloride solution. Its colour and reactions agreed with those of a chalkone (V). Yield, 60 mg. (Found: C, 56·6; H, 4·5; $C_{17}H_{15}O_4Br$ requires C, 56·2; H, 4·1%.)

The ethyl acetate mother liquors left from the crystallisation of bromoflavanone (IV) and containing the more soluble portion was evaporated and the residue (containing VI) was treated with alcoholic sodium hydroxide (30 c.c., 2%) for 2 hours and then the solution was diluted with water when pale-yellow needles separated out. This product was filtered, washed with water in order to free it from alkali, dried at room temperature and then crystallised from benzene 5 times when very pale-yellow needles melting at 250–2° were obtained. The substance (VII) gave Lassaigne's test for bromine. Yield, 20 mg. (Found: C, 57·0; H, 4·1; $C_{17}H_{13}O_4Br$ requires C, 56·5; H, 3·6%.)

(3) *Naringenin Acetate* (*VIII*)

(*a*) *Preparation of Acetate.*—Naringenin (1·6 g.) was dissolved in pyridine (5 c.c.), cooled in an ice-bath and acetyl chloride (1·3 c.c.) added from a dropping funnel very slowly with stirring by means of a magnetic stirrer. At the end of the addition the mixture became semi-solid due to the separation of pyridine hydrochloride and more pyridine (5 c.c.) was added. Stirring was continued for 1 hour more and then the vessel was corked well and kept in the refrigerator. Next day ice (about 50 g.) was added and the mixture stirred when a semi-solid mass separated out. It was taken up in ether, dried over anhydrous sodium sulphate and the solvent was removed, when again a semi-solid residue was left behind. There was a strong smell of pyridine. Hence it was treated with ether-petroleum ether mixture when it turned into a colourless crystalline solid. It then crystallised from ethyl acetate-petroleum ether mixture in colourless, starry bunches of long needles sintering and becoming glassy at 80–82° and finally melting at 90–92°. Yield, 1·1 g. (Found: C, 63·3; H, 4·5; $C_{21}H_{18}O_8$ requires: C, 63·3; H, 4·5%.)

(*b*) *Reaction with N-Bromo-succinimide.*—The above acetate (0·33 g.), N-bromo-succinimide (0·15 g.) and benzoyl peroxide (0·01 g.) were dissolved

in anhydrous carbon tetrachloride (40 c.c.) and the mixture was refluxed on a steam-bath. The solution became pale-brown in about an hour but only a very small amount of brownish precipitate had separated out. More of N-bromo-succinimide (0·1 g.) was, therefore, added when the solution became reddish-brown and refluxed for further 2 hours. More of the reddish-brown precipitate separated out and it gradually became colourless and crystalline. The colour of the reaction mixture became permanent pale-brown at the end of the reaction. The mixture was then cooled and the solid (succinimide) was filtered off. When the solvent was removed from the filtrate a very pale-brown solid was left behind. It was washed thrice with hot water, dried at room temperature and then crystallised from ethyl acetate-petroleum ether mixture when fine, pale-yellow needles melting at 181–2° were obtained. It did not give Lassaigne's test for bromine. Yield, 0·1 g. (Found: C, 63·4; H, 4·3; $C_{21}H_{16}O_8$ requires C, 63·6; H, 4·0%.) The substance was found to be identical with apigenin acetate (IX) and the mixed melting point with an authentic sample was undepressed.

The colourless residue (VIII *a*, 40 mg.) from the mother liquors (of IX) was dissolved in aqueous alcoholic sodium hydroxide solution (1%, 10 c.c.) and warmed for 5 minutes. The solution was then cooled, diluted with water and acidified with dilute hydrochloric acid when a yellow solid separated out. It was taken up in ether, the ether extract dried over anhydrous calcium chloride and the solvent was then evaporated. A yellow solid was left behind. It crystallised from ethyl acetate in rectangular prisms melting at 342–5°. A mixed melting point with an authentic sample of apigenin was undepressed.

Summary

Use of N-bromo-succinimide for the conversion of flavanones into flavones is investigated. 7-Methoxy-flavanone undergoes bromination in the 3-position and on treatment with alcoholic sodium hydroxide solution gives rise to a good yield of 7-methoxy-flavone. On the other hand, 5:7-dimethoxy flavanone suffers nuclear bromination more prominently and yields a mixture of products containing 8-bromo-5:7-dimethoxy-flavanone and the 3:8-dibromo compound. Naringenin acetate yields as the major product apigenin acetate, as the result of substitution in the 3-position and subsequent elimination of hydrogen bromide; the other product is 3-bromo-naringenin acetate which undergoes conversion into apigenin with alkali. Acetates therefore appear to be the most convenient derivatives for this reaction.

REFERENCES

1. Narasimhachari and Seshadri — *Proc. Ind. Acad. Sci.*, 1949, **30 A**, 151.
2. Kostanecki and Lampe .. *Ber.*, 1904, **37**, 3167–8.
3. Zemplen and Bögnar .. *Ibid.*, 1943, **76**, 452.
4. Schmid and Karrer .. *Helv. Chim. Acta*, 1946, **29**, 573.
5. Sorkin, *et al.* .. *Ibid.*, 1948, **31**, 65.
6. Erlenmeyer and Grubenmann *Ibid.*, 1947, **66**, 297.
7. Asahina and Inubuse .. *Ber.*, 1928, **61 B**, 1514–6.
8. Meystre *et al.* .. *Helv. Chim. Acta*, 1945, **28**, 1252; 1945, **28**, 1497; 1946, **29**, 627.

Note added in the Proof.—After submitting this paper for publication we have come across the paper of Lorette *et al.*, *C. A.*, 1952, **46**, 1540–41, in which they have used N-bromo-succinimide and pyridinium bromide perbromide for the bromination of acetyl hesperidin and naringin. The bromination products were directly treated with alkali and the resulting flavone glycosides characterised. They have also recorded the need fo the peroxide catalyst.

THERMAL EXPANSION OF CRYSTALS AT LOW TEMPERATURES—Part I. SUGAR

By A. K. Sreedhar

(From the Department of Physics, Indian Institute of Science, Bangalore)

Received May 23, 1952

(Communicated by Prof. R. S. Krishnan, F.A.SC.

1. Introduction

The study of thermal expansion of crystals, especially those of monoclinic and triclinic varieties has been very meagre. The crystals of monoclinic and triclinic forms present considerable difficulties. On account of the anisotropy of the expansion, four sets of experiments for monoclinic and six for the triclinic are necessary to fix the dilatation ellipsoid and even after fixing the ellipsoid, three more experiments have to be done along the three principal directions of the ellipsoid if one wants to investigate the variation of the coefficient of expansion with termeprature.

Most of the monoclinic and triclinic crystals which are at the disposal of the author are artificially grown and contain water of crystallization besides having low melting points. Thus their thermal properties can only be investigated at lower temperatures. With this idea in view a low temperature expansion apparatus, with which the expansion of crystals can be investigated from liquid-air temperature to room temperature was constructed and the results of a monoclinic crystal, cane sugar, are presented here.

The crystals of cane sugar were artificially grown and can be had in fairly big sizes with well-developed faces. The crystal has the planes (100), (110) and (10$\bar{1}$) well formed and hence its crystallographic axes can be easily identified. Groth has given the axial ratios as $1{\cdot}2595 : 1 : 0{\cdot}8782$ with $\beta = 103° 30'$.

2. Experimental Technique

In the present work the well-known Fizeau interferometric method as modified by Merritt (1933) and Saunders (1939) was employed. The latter has described in great detail the entire experimental procedure to be followed in order to obtain results with the greatest accuracy.

The low temperature apparatus (see Fig. 1) follows with suitable modifications that described by Adenstadt in his classic experiments. It consisted

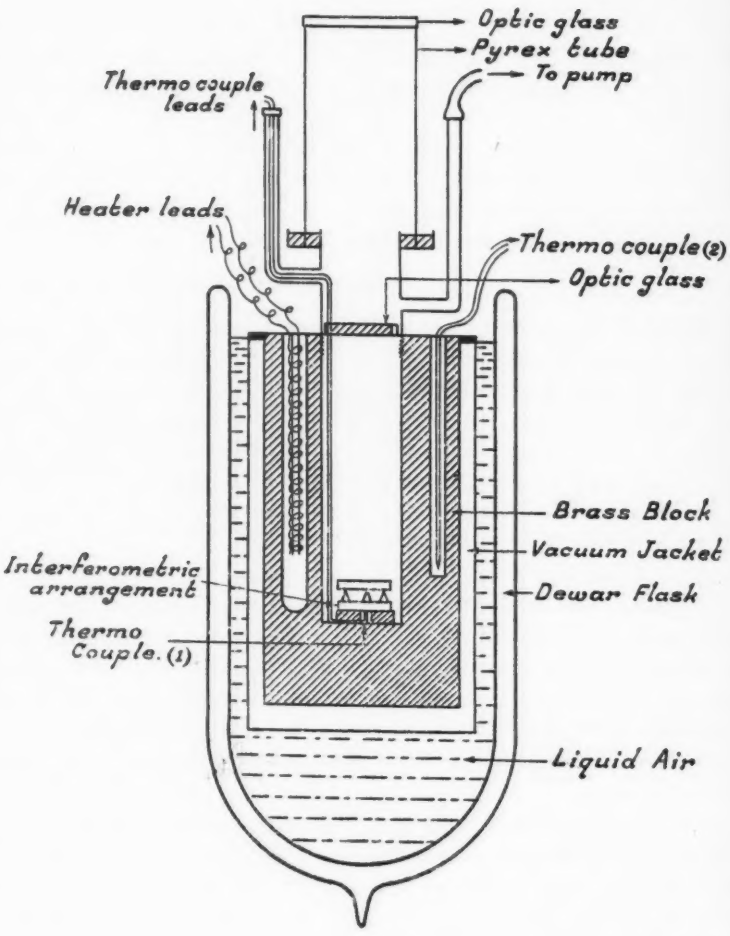

FIG. 1

of a heavy brass block (4 kgm.) which was surrounded by a vacuum jacket. The brass cylinder had three holes bored into it. The central big one holds the interferometric arrangement and was covered by an optic glass plate. It was then closed by a pyrex tube the top of this tube being closed by another optic glass plate. The whole interior was then evacuated through a side tube to a pressure of 2–3 mm. of mercury. This small pressure was enough to ensure good thermal contact between various parts of the interferometer but at the same time was low enough to avoid condensation of

carbon dioxide and moisture on the plates. Correction due to the variation of refractive index of air with temperature could be neglected on account of the smallness of pressure.

The temperature of the specimen was indicated by a calibrated copper constantan thermocouple. A Leeds and Northrup potentiometer in conjunction with a standard Weston Cadmium cell and a sensitive galvanometer was used to measure thermocouple voltages. This was sensitive up to a microvolt.

Of the other two holes in the brass block, one contained a 300 watt insulated heating element and the second another copper constantan thermocouple. The entire low temperature arrangement could be immersed in a bath of liquid air whose level could be adjusted by a screw stand. By adjusting the degree of vacuum in the outer jacket and the current in the heating element any desired rate of heating or cooling might be obtained. In the present work the rate was 1° C. per minute this being found sufficient to ensure good thermal equilibrium between various parts of the interferometer and the thermocouple.

3. Preparation of the Specimens and Procedure for Monoclinic Systems

In the crystal of cane sugar, the (100), (001) and (110) planes are well developed and hence it is easy to identify the crystallographic axes. Since one of the principal axes of the dilatation ellipsoid must coincide with the diad axis of the crystal, *i.e.*, the *b*-axis, a measurement of the expansion along the *b*-axis directly gives one of the three principal expansion coefficients, α_{22}. Hence three pyramids were cut with their vertices pointing along the *b*-axis and the expansion was measured from $-150°$ C. to room temperature. The other two principal axes lie on the (010) plane of the crystal and in order to fix them measurements in three different directions in the (010) plane are required. The relative positions of the crystallographic axes, *a*, *c*, the principal expansion axes OX_1, OX_3 and the arbitrary direction OX_3', along which the expansion is measured are shown in Fig. 2. Then if α_{33}' is the expansion along OX_3' we have the relation

$$\alpha_{33}' = A + B \cos 2\xi + C \sin 2\xi, \qquad \text{(Wooster)}$$

where A, B and C are given by

$$A = \frac{\alpha_{11} + \alpha_{33}}{2}; \quad B = \frac{\alpha_{11} - \alpha_{33}}{2} \cos 2\psi \text{ and } C = -\frac{(\alpha_{11} - \alpha_{33})}{2} \sin 2\psi$$

ψ and ξ are those indicated in Fig. 2. α_{11} and α_{33} are the principal expansions, *i.e.*, expansions along OX_1 and OX_3. Since α_{33}' and ξ are measurable,

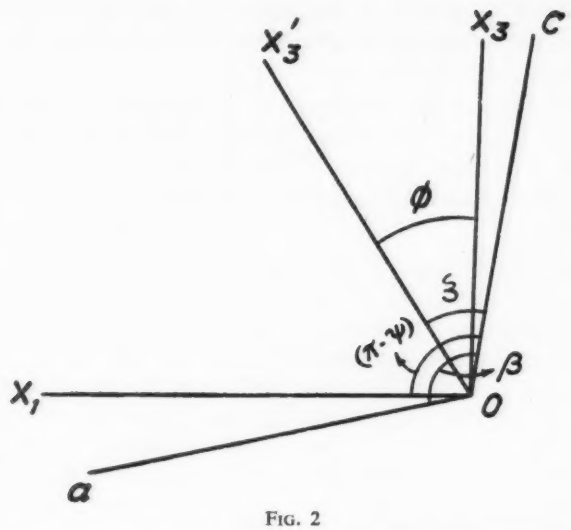

FIG. 2

three sets of measurements along three different arbitrary directions give three simultaneous equations from which A, B and C may be found. Solving for ψ, α_{11} and α_{33} we find $-\tan 2\psi = C/B$; $\alpha_{11} = A + B/\cos 2\psi$

and $\alpha_{33} = (A - B)/\cos 2\psi$.

Thus all the required information, *viz.*, α_{11}, α_{33} and ψ may be obtained. In the experiment the three directions chosen were

(i) along the *c*-axis of the crystal, *i.e.*, $\xi = 0$,

(ii) along the *a*-axis of the crystal, *i.e.*, $\xi = \beta = 103° 30'$,

(iii) along the bisector of *a* and *c* axes, *i.e.*, $\xi = \beta/2$.

The expansions were measured along these three directions and using Wooster's formula, above, α_{11}, α_{33} and ψ were calculated at room temperature at which β is known. After thus fixing the dilatation ellipsoid two more sets of pyramids, now along OX_1 and OX_3 were cut and the expansion along theses were measured from $-160°$ C. upto room temperature.

4. RESULTS

The coefficients of thermal expansion along α_{11}, α_{33} and α_{22} are given in Tables I, II and III respectively against temperature. The variations of α_{11}, α_{22} and α_{33} with temperature are also shown graphically in Fig. 3. Unfortunately due to the difficulty of interpretation of the results due to the variation of β with temperature no determination was made along any other arbitrary direction.

TABLE I

Coefficient of linear expansion of sugar along OX_1 (α_{11})

Temperature °C.	$\alpha_{11}\times10^{-6}$	Temperatur °C.	$\alpha\times10^{6}$
−163	20·66	−43	26·29
−133	22·35	− 9	27·09
−101	23·11	25	29·18

TABLE II

Coefficient of linear expansion of cane sugar along OX_3 (α_{33})

Temperature °C.	$\alpha_{33}\times10^{6}$	Temperature °C.	$\alpha_{33}\times10^{6}$
−123	19·59	−63	31·88
−103	24·17	−43	35·51
− 83	28·07	0	41·96

TABLE III

Coefficient of linear expansion of cane sugar along b-*axis of the crystal,* i.e., α_{22}

Temperature °C.	$\alpha_{22}\times10^{6}$	Temperature °C.	$\alpha_{22}\times10^{6}$
−100	16·34	−58	23·3
− 88	18·41	−23	30·11
− 18	20·0	− 3	36·67

With angle $\psi = -23° 3\frac{1}{2}'$. at room temperature,

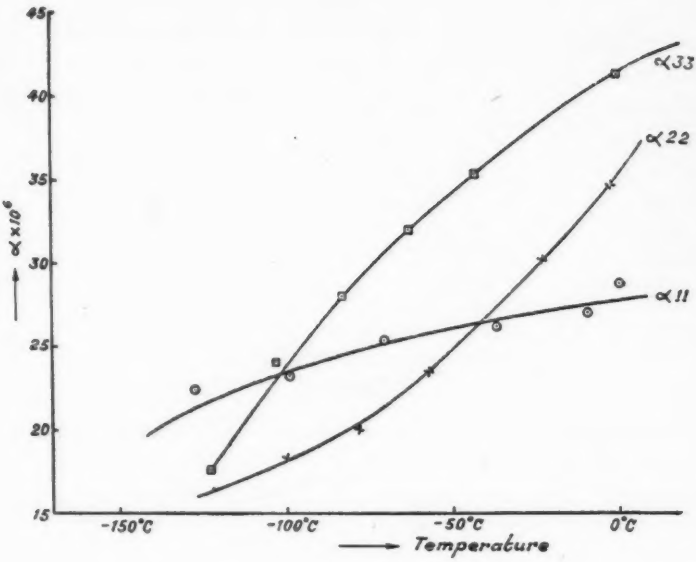

FIG. 3

5. DISCUSSION

From a perusal of the results given above it is obvious that the variation of α with temperature is fairly high especially at lower temperatures and the values show a tendency towards saturation at higher temperatures. Unfortunately data regarding variation of elastic constants, etc., are not available so that no comparison can be effected between the expansion coefficients and the elastic constants. At zero ° C. the values of α_{11}, α_{22} and α_{33} are in the ratio of 29·18 : 36·67 : 41·96, thus showing the high anisotropy of the crystal. These values are approximately inversely proportional to the axial ratios given by Groth. One peculiarity which the graph shows is that while the curves for α_{11} and α_{33} are convex that for α_{22} is of the opposite nature. At about $-40°$ C. $\alpha_{11} = \alpha_{22} = 26·5$ and at about $-106°$ C. $\alpha_{11} = \alpha_{33} = 23·2$ and at this temperature the expansion in the (010) plane should be isotropic.

In conclusion the author expresses his gratitude to Prof. R. S. Krishnan for suggesting the problem and for his constant interest in the work. My thanks are also due to the Director of the Sugar Technological Institute, Cawnpore, for kindly presenting the cane sugar crystals.

6. Summary

The thermal expansion of a typical monoclinic crystal has been measured thoroughly using a low temperature apparatus and results obtained are shown in Fig. 3. It is found that in the case of cane sugar the anisotropy of expansion is fairly high especially at low temperatures while at room temperatures it is not so anisotropic.

References

Adenstadt .. *Ann. der Phy.*, 1936, **26**, 69.

Fizeau .. *Ann. Chim. Phy.*, 1884, **2** (4), **146**.
Ibid., 1886, **8**, 335.

Groth .. *Chem. Crystallography*, Vol. **3**.

Merritt .. *J. Res. Bur. Stds.*, 1933, **10**, 59.

Saunders .. *Ibid.*, 1939, **23**, 179.

Wooster .. *Crystal Physics*, 1949.

PHOTOCHEMICAL AFTER-EFFECT IN THE BROMINE-OXALATE REACTION

By B. B. Lal, F.A.Sc.

(*Chemical Laboratories, Department of Archæology, Dehra Dun*)

Received in revised form, February 10, 1952

Introduction

Dhar[1] (1925) discovered that a mixture of oxalic acid and bromine exposed to light for a short time and then brought back into the dark shows a greater rate of bromine reduction than a mixture that has not been illuminated. The photochemical after-effect was found to be of a short duration. The unimolecular velocity constants after irradiation approached the dark reaction rate in about half an hour from the time of darkening. No bromide was used in the reaction mixture.

The reaction between potassium oxalate and bromine has formed the subject of extensive studies by Bhattacharya and Dhar[2] (1929), and Bhattacharya, Prakash and Dhar[3] (1932). These authors studied the reaction between bromine and neutral potassium oxalate, and measured the quantum efficiency of the photochemical reaction in the mercury arc light, as well as the reaction velocity and light absorption under varying conditions. Griffith, Mckeown and Winn[4] (1933) have discussed at length the photochemical reactions between bromine and neutral oxalate and free oxalic acid. None of these workers, however, made any observation about the photochemical after-effect in these reactions. With the exception of Dhar's[1] preliminary experiment referred to above, there is no record in the literature of work on the photochemical after-effect in the oxalic acid-bromine reaction. It was, therefore, thought desirable to study this reaction in detail in order to throw some light on the mechanism of the after-reaction. The present paper contains some observations on the photochemical after-effect in the reaction between free oxalic acid and bromine. It is significant to note that the reaction between bromine and neutral potassium oxalate has also been found by the author to exhibit a marked photochemical after-effect of several hours' duration.

Experimental

Kahlbaum's analytical reagents were employed in this investigation. The experiments were conducted in pyrex glass bulbs, duly cleaned and steamed before use. The experiments on the oxalic acid-bromine reaction were conducted at 35° C. This reaction has been found by Dhar[1] to be approximately unimolecular with respect to bromine. The dark reaction

produces hydrobromic acid which exerts a retarding effect on the rate of bromine reduction. In order to minimise the fall in the unimolecular velocity constants with the progress of the reaction, an excess of potassium bromide was employed in the reaction mixture. The change in bromine concentration was determined from time to time by adding an excess of potassium iodide to 5 c.c. of the reaction mixture in the dark and titrating the liberated iodine with standard thiosulphate solution. The reaction between oxalic acid and iodine is negligible under the conditions of these experiments. Due care was taken to prevent the action of light on the reaction mixture during titration.

The oxidation reaction between oxalic acid and hypobromous acid has not been considered, because under the conditions of the experiments described here, the formation of hypobromous acid by hydrolysis

$$Br_2 + H_2O \rightleftharpoons HBrO + HBr$$

is negligible. Due to the presence of hydrogen and bromide ions, the hydrolytic equilibrium is suppressed with the disappearance of hypobromous acid. All the experiments described here have been carried out in the presence of a large excess of bromide ions. The hydrolysis constant of the above equilibrium is of the order[5] of 10^{-8} and even in the absence of such an initial excess of bromide ion as used in these experiments the formation of hypobromous acid is practically negligible.

Fig. 1 shows the results obtained by using N/10 oxalic acid, N/120 bromine and N/5 potassium bromide. Curve 1 shows the course of the

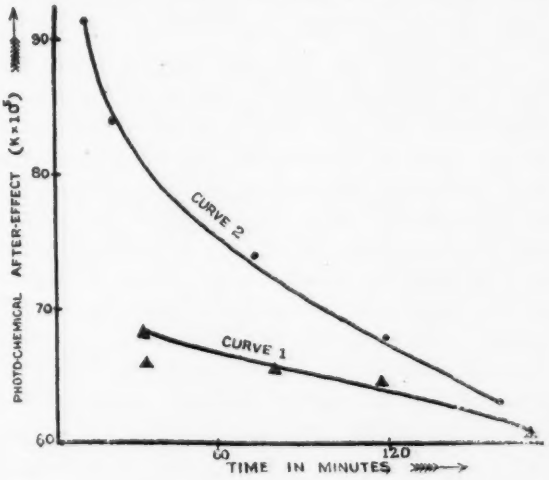

FIG. 1

dark reaction, and Curve 2 shows the course of bromine reduction after illumination of the reaction mixture for 30 minutes by the light (filtered through water) of a 500-watt gas-filled filament lamp operated at 220 volts. The distance between the reaction vessel and the lamp was 50 cm. These results are recorded in Tables I–II. The velocity constant has been calculated according to the unimolecular formula, $K = 1/t \log a/a-x$, where 't' is the time in minutes and 'a' the initial concentration of bromine in terms of c.c. of thiosulphate, and 'x' the change in time 't'.

TABLE I

In the dark throughout

t	$a-x$	K.10^6
0	8·30	..
52	7·65	681
54	7·30	664
132	6·80	656
196	6·20	646
287	5·50	609

TABLE II

Exposed to light for 30 mts. and then measured bromine reduction in the dark

t	$a-x$	K.10^6
0	6·50	..
15	6·30	907
37	6·05	841
81	5·60	799
120	5·30	738
200	4·75	681
270	4·40	627

As the object of these experiments was to study the photochemical after-effect, no attempt was made to study the light absorption and quantum efficiency. These aspects of the reaction have been extensively studied by Dhar and co-workers[1,2,3] and Griffith, *et al.*[4]

It may be emphasized that the photochemical after-effect is essentially a dark reaction initially stimulated by irradiation for a short time. From these experiments it is seen that the photochemical after-effect persists for over four hours. The activity in the pre-illuminated reaction mixture diminishes first rapidly and later on gradually until the velocity constants approach the dark reaction rate. The course of the after-reaction cannot be represented by any kinetic equation. It appears that in the primary light reaction some activated intermediate product is formed which causes the measured after-effect and at the same time disappears in other ways. The total change in bromine concentration cannot be represented by any simple formula. Similar 'decay curves' have been obtained in the photochemical after-effect in the reaction between iodine and oxalate[6] (1939).

Irradiation of $H_2C_2O_4$-Br_2-KBr mixture by quartz mercury vapour lamp gave the results that have been shown in Fig. 2 and recorded in Tables

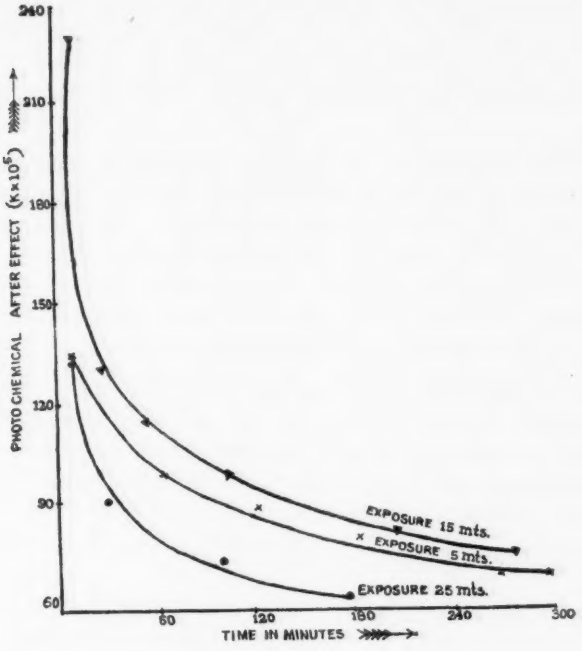

FIG. 2

III–V. The 'decay curves' show that there is a rapid fall in activity just after cutting off the illumination, so that it has been largely reduced by the time the first reading for the photochemical after-effect is taken. The results also show that the photochemical after-effect increases with increasing periods of pre-illumination up to a certain stage. When the

TABLE III

Exposure 3 *mts.*

t	$a-x$	K.10^5
0	6·50	..
10	6·30	136
63	5·65	96
120	5·05	91
180	4·65	81
300	4·05	69

TABLE IV

Exposure 15 *mts.*

t	$a-x$	K.10^5
0	4·80	..
10	4·55	232
25	4·45	131
50	4·20	116
101	3·80	100
200	3·40	84
275	3·10	76

TABLE V

Exposure 25 *mts.*

t	$a-x$	K.10^5
0	3·30	..
10	3·20	134
30	3·10	90
97	2·80	74
174	2·55	64

irradiation is prolonged for some time, the after-effect shows a diminution. The observed diminution in the photochemical after-effect may be due to the retarding effect of hydrobromic acid which is produced in considerable concentration in the course of the reaction. This point is being investigated.

When the concentration of potassium bromide is diminished, the dark reaction becomes more rapid, and no after-effect of illumination can be observed when the concentration of potassium bromide is sufficiently reduced. It appears that the photochemical after-effect is very largely masked by the rapid rate of the dark reaction, and the former can be detected only when the dark rate has been considerably reduced by employing larger concentrations of potassium bromide.

It was noticed that when the original concentration of bromine in $H_2C_2O_4$-Br_2-KBr mixture was restored in the dark immediately after the complete photo-reduction of bromine, the rate of reaction now obtained with added bromine was slightly lower than the dark rate and no ' secondary after-effect[6]' could be observed.

Potassium oxalate and bromine

A marked photochemical after-effect was noticed for the first time in the reaction between neutral potassium oxalate and bromine. They react rapidly at room temperature in the dark, and no photochemical after-effect could be detected at such temperatures. When, however, the dark reaction was damped by employing a large excess of potassium bromide and by carrying out the experiments at a lower temperature, a marked after-effect of illumination was observed.

Dark reaction.—The dark reaction between bromine and neutral potassium oxalate has been studied by a large number of workers. The dark reaction has been found to be unimolecular with respect to bromine. It has been established by the author that the reaction between potassium oxalate and bromine in the presence of a large excess of potassium bromide and oxalate is unimolecular with respect to bromine. In the absence of added bromide and considerable excess of oxalate the dark reaction is complex, but in the present study this complexity has been largely avoided by using large concentrations of both oxalate and bromide and isolating the reaction. The dark reaction has been studied under different conditions of temperature and concentration. Some typical experiments have been recorded in Tables VI–VIII. The concentrations were N/10 $K_2C_2O_4$, N/5 KBr and N/120 Br_2.

TABLE VI

Temp. 0·3°–0·8° *C.*

t	*a*−*x*	K.10⁶
0	7·70	..
60	7·45	238
120	7·25	218
206	6·95	216
252	6·65	253

TABLE VII

Temp. 10° *C.*

t	*a*−*x*	K.10⁵
0	6·80	..
15	6·35	198
37	5·85	177
64	5·20	182
105	4·45	175
179	3·10	191

TABLE VIII

Temp. 25° *C.*

t	*a*−*x*	K.10⁴
0	7·20	..
13	3·60	232
19	2·40	251
24	1·80	245

The above experiments show that the unimolecular velocity constants ($K = 1/t \log a/a - x$) are fairly constant and the dark reaction is unimolecular with respect to bromine.

Photochemical after-effect.—The photochemical after-effect was studied by irradiating the reaction mixture at 0·3°–0·8° C. in a glass thermostat placed at a distance of 50 cm. from the lamp (500-watt gas-filled filament lamp operated at 220 volts). The results are recorded in Tables IX–X.

TABLE IX

N/10 $K_2C_2O_4$, *N*/4 *KBr*, *N*/120 Br_2

t	*a*−*x*	K.10⁶	
0	7·30	..	
60	7·15	150	138
120	7·05	126	

Illumination 10 mts.			After-effect
152	4·40	..	..
182	4·30	333	195
312	4·05	225	87
420	3·95	175	37

TABLE X

N/8 *KBr*, *other conditions same as in Table IX*

t	*a*−*x*	K.10⁶	
0	7·40	..	
60	7·15	248	251
120	6·95	253	

Illumination 10 mts.			After-effect
172	3·20	..	..
213	3·10	334	83
330	2·85	318	67
421	2·70	294	43
540	2·50	280	29

In Tables IX–X, the after-effect has been evaluated by subtracting the rate of the dark reaction from the rate after irradiation. The first three readings above the line give dark reaction rates which were found to be in agreement with those obtained in dark reactions studied independently. The readings after switching off the light have been taken so long as the after-effect rates are distinctly higher than the dark rate. It is found that a marked after-effect of illumination is obtained after a short illumination (10 mts.) by the light of 500-watt filament lamp, and the after-effect persists for several hours as in the case of the oxalic acid-bromine reaction. It is clear from Table X that when the bromide concentration is reduced, the dark reaction becomes more rapid and the photochemical after-effect is considerably diminished. It was found that with N/2 potassium oxalate, and N/8 potassium bromide, the reduction of bromine in the dark was very rapid ($K.10^5 = 121$), and no after-effect could be detected under these conditions.

DISCUSSION

It is not possible at this stage to explain the mechanism of the photochemical after-effect in the oxalic acid-bromine and the oxalate-bromine reactions. From the experimental results obtained, it appears that some reactive intermediate product is formed by the primary photochemical reaction between bromine and oxalate ion which continues its active influence after darkening, thus causing the photochemical after-effect. The velocity constant at any time in the after-reaction would, therefore, represent the mass of this active product at that time. This reacts with bromine more rapidly than the oxalate ion C_2O_4'' and causes the photochemical after-effect, while decaying spontaneously in other ways. Abel and Schmidt[7] (1935) reported the existence of the univalent oxalato ion C_2O_4' of long life in the iodine-oxalate reaction, and suggested that the photochemical after-effect in this reaction is an evidence of the existence of this ion. This intermediary product which was suspected on kinetic grounds by Abel,[8] Schmidt and Retter (1932) had been originally postulated by Berthoud (1924)[9] in the photochemical reaction between potassium oxalate and iodine. Abel, *et al.*[8] further concluded from kinetic measurements on the iodine-oxalate reaction that the photo-formation and accumulation of univalent oxalato ion C_2O_4' of long life following irradiation of the reaction mixture is responsible for enhanced activity after subsequent darkening, the half-ion continuing its active influence on iodine and at the same time decaying spontaneously in other ways. More recently a detailed investigation of the marked photochemical after-effect of long duration in the iodine-oxalate reaction has been carried out[6] (1940), and a mechanism has been suggested

dispensing with the assumptions about the existence of activated molecules of long life as postulated by Mukerji and Dhar[10] (1928) and depending solely upon a simple extension of the Berthoud chain mechanism (involving the univalent oxalato ion C_2O_4') for the oxalate-iodine photo-reaction.

Experimental observations described in the present paper indicate that a close similarity exists between the photochemical after-effect in the iodine-oxalate reaction[6] and the photochemical after-effect between bromine and oxalic acid or potassium oxalate under discussion. As already stated the formation of the univalent oxalato ion C_2O_4' has been postulated by Berthoud[9] (1924) as a part of the mechanism involved in the bromine-oxalate photo-reaction. If it is assumed that the univalent oxalato ion so produced in the light reaction reacts with bromine more slowly than the rate at which it is formed in light, so that an excess of this active ion accumulates, the photochemical after-effect can be accounted for by the high reactivity towards bromine of this ion which carries on the chain when the illumination is withdrawn. The variation in the magnitude of the photochemical after-effect with the period of pre-illumination shows that the formation of C_2O_4' in light is faster than the rate at which they are used up, so that an excess of this ion accumulates depending on the period of pre-illumination. A similar mechanism has been postulated in the reaction between oxalic acid and potassium permanganate involving the half-ion C_2O_4' (1943)[11].

The failure to detect the 'secondary after-effect' (MacMahon and Lal, 1940)[6] in this reaction suggests that when all the bromine is used up in the light reaction, the univalent oxalato ions left behind after cutting off the illumination rapidly disappear by self-combination:

$$C_2O_4' + C_2O_4' = 2\,CO_2 + C_2O_4''$$

This self-combination of the oxalato ion has been assumed to be responsible for the decay of the photochemical after-effect in the iodine-oxalate reaction.[6] The decay of the photochemical after-effect in reactions involving bromine may also be ascribed to the gradual disappearance of the chain carrier C_2O_4' in the above manner.

A complete elucidation of the mechanism of the photochemical after-effect in this reaction must await the results of further research. Experiments are already in progress in this direction. The above tentative mechanism has been suggested in the absence of further experimental evidence.

Summary

A marked photochemical after-effect has been observed in the oxalic acid-bromine reaction in the presence of excess of potassium bromide.

The after-effect persists for several hours after cutting off the illumination, and increases with increasing periods of pre-illumination up to a certain stage. If the illumination is continued for longer periods the after-effect shows a diminution. The study of the retarding action of hydrobromic acid which is a product of the reaction may explain this diminution. When the bromine that has been photochemically removed in the light reaction is restored in the end solution in the dark immediately after the completion of the photo-reaction, no 'secondary after-effect' is observed.

Under suitable conditions the photochemical reaction between potassium oxalate and bromine is followed by a marked photochemical after-effect which persists for several hours. No 'secondary after-effect' could be detected in this reaction.

The 'decay' of the photochemical after-effect is very rapid just after the illumination is withdrawn and is relatively slower afterwards. It appears that the active intermediate product formed in the light reaction reacts with bromine giving the photochemical after-effect and is at the same time destroyed in other ways.

A tentative mechanism of these after-effects has been suggested involving the formation of the univalent oxalato ion C_2O_4'.

The author's best thanks are due to Professor P. S. MacMahon, Lucknow University, for his kind interest in this work.

BIBLIOGRAPHY

1. Dhar .. *Jour. Ind. Chem. Soc.* 1925, **2,** 281.
2. Bhattacharya and Dhar .. *Ibid.*, 1929, **6,** 523.
3. Bhattacharya, Prakash and Dhar .. *Z. Anorg. Allgem. Chem.*, 1932, **209,** 139-44.
4. Griffith, Mckeown and Winn .. *Trans. Farad. Soc.*, 1933, **29,** 369-86.
5. Mellor .. *A Comprehensive Treatise on Inorganic and Theoretical Chemistry*, 1922, **2,** 78.
6. MacMahon and Lal .. *Jour. Ind. Chem. Soc.*, 1940, **17** (7), 438.
7. Abel and Schmidt .. *Naturwiss.*, 1935, **23,** 501.
8. Abel, Schmidt and Retter .. *Zeit. Physikal. Chem.*, 1932, **163 A,** 53.
9. Berthoud .. *Helv. Chim. Acta.*, 1924, **7,** 307.
10. Mukerji and Dhar .. *Jour. Ind. Chem. Soc.*, 1928, **5,** 203.
11. MacMahon and Lal .. *Ibid.*, 1943, **20,** 143-52.

720-52 Printed at The Bangalore Press, Bangalore City, by C. Srinivasa Rao, Superintendent, and Published by The Indian Academy of Sciences, Bangalore